GeoScienceWorld
Lithosphere
VoVolume 2020, Article ID 8850336, 24 pages
https://doi.org/10.2113/2020/8850336

Lithosphere

Research Article

Pulsed Mesozoic Deformation in the Cordilleran Hinterland and Evolution of the Nevadaplano: Insights from the Pequop Mountains, NE Nevada

Andrew V. Zuza,[1] Charles H. Thorman,[2] Christopher D. Henry,[1] Drew A. Levy,[1] Seth Dee,[1] Sean P. Long,[3] Charles A. Sandberg,[2] and Emmanuel Soignard[4]

[1]*Nevada Bureau of Mines and Geology, University of Nevada, Reno, NV 89523, USA*
[2]*Emeritus, Lakewood, CO 80228, USA*
[3]*School of the Environment, Washington State University, Pullman, WA 642812, USA*
[4]*Eyring Materials Center, Arizona State University, Tempe, AZ 85287, USA*

Correspondence should be addressed to Andrew V. Zuza; azuza@unr.edu

Received 27 August 2019; Accepted 31 January 2020; Published 29 July 2020

Academic Editor: Laurent Godin

Mesozoic crustal shortening in the North American Cordillera's hinterland was related to the construction of the Nevadaplano orogenic plateau. Petrologic and geochemical proxies in Cordilleran core complexes suggest substantial Late Cretaceous crustal thickening during plateau construction. In eastern Nevada, geobarometry from the Snake Range and Ruby Mountains-East Humboldt Range-Wood Hills-Pequop Mountains (REWP) core complexes suggests that the ~10–12 km thick Neoproterozoic-Triassic passive-margin sequence was buried to great depths (>30 km) during Mesozoic shortening and was later exhumed to the surface via high-magnitude Cenozoic extension. Deep regional burial is commonly reconciled with structural models involving cryptic thrust sheets, such as the hypothesized Windermere thrust in the REWP. We test the viability of deep thrust burial by examining the least-deformed part of the REWP in the Pequop Mountains. Observations include a compilation of new and published peak temperature estimates ($n = 60$) spanning the Neoproterozoic-Triassic strata, documentation of critical field relationships that constrain deformation style and timing, and new $^{40}Ar/^{39}Ar$ ages. This evidence refutes models of deep regional thrust burial, including (1) recognition that most contractional structures in the Pequop Mountains formed in the Jurassic, not Cretaceous, and (2) peak temperature constraints and field relationships are inconsistent with deep burial. Jurassic deformation recorded here correlates with coeval structures spanning western Nevada to central Utah, which highlights that Middle-Late Jurassic shortening was significant in the Cordilleran hinterland. These observations challenge commonly held views for the Mesozoic-early Cenozoic evolution of the REWP and Cordilleran hinterland, including the timing of contractional strain, temporal evolution of plateau growth, and initial conditions for high-magnitude Cenozoic extension. The long-standing differences between peak-pressure estimates and field relationships in Nevadan core complexes may reflect tectonic overpressure.

1. Introduction

The evolution of orogenic plateaus is an important topic in continental tectonics that impacts society (e.g., seismicity and natural resources; e.g., [1–5]), tectonic-related climate change [6, 7], Earth's geochemical cycling [8, 9], and crust-mantle coupling [10–12]. Plateau research largely focused on the modern Andes and Tibet has progressively refined their growth timescales (e.g., [13–15]) (Figure 1), and concepts learned from these regions can be applied to other ancient orogens. However, the evolution of the Mesozoic-early Cenozoic Nevadaplano [16] is enigmatic, primarily due to its late Cenozoic extensional dismemberment. Preferred mechanisms of Cenozoic extension hinge on the tectonic history of the preexisting Mesozoic orogenic plateau, and whether plateau collapse is fundamentally governed by

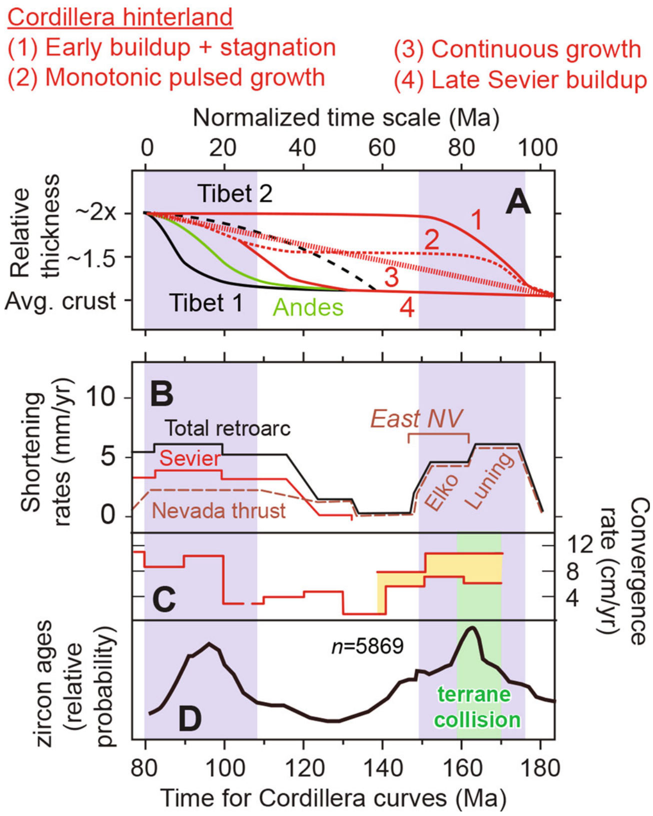

Figure 1: (a) Plateau growth curves for Tibet (2 options; [13, 15]), Andes [14], and the North American Cordillera (dashed red curves are favored in this study). (b) Cordilleran retroarc shortening rates [56] modified to include Elko Orogeny deformation ([32, 61]; this study). Purple background shadings are Jurassic and Cretaceous phases of deformation. (c) North America-Farallon convergence rates from Yonkee and Weil [56] based on Seton et al. [166] and Engebretson et al. [167]. (d) Detrital zircon ages from the Sierra Nevada ([139] and references therein) and timing of terrane accretion [136].

boundary conditions (i.e., relative plate motion), internal body forces (i.e., gravitational collapse), or a combination remains unclear (e.g., [17, 18]).

Cenozoic exhumation of Cordilleran core complexes has exposed a record of Mesozoic contraction and crustal thickening (e.g., [19–21]). Geobarometric studies from the Ruby Mountains-East Humboldt Range-Wood Hills-Pequop Mountains (REWP) and Snake Range core complexes of eastern Nevada suggest the 10–12 km thick Neoproterozoic-Triassic passive-margin sequence was buried to great depths (>30 km) by the Late Cretaceous and later exhumed to the surface via high-magnitude Cenozoic extension [22–25]. This implies substantial tectonic burial and associated crustal thickening, which was probably part of orogenic plateau development [26, 27] that is indirectly supported by geochemical proxies [26, 28, 29].

Geobarometric data from the REWP and Snake Range core complexes have been reconciled with structural models for regional burial under cryptic thrust sheets that duplicate Neoproterozoic-Paleozoic stratigraphy [24, 30]. Specifically for the REWP, the Windermere thrust sheet was hypothesized to bury rocks in the Wood Hills and Pequop Mountains to depths in agreement with geobarometric studies [30]. To date, no field evidence for the Windermere thrust has been found, which has spurred a debate over the timing and magnitude of Mesozoic contraction (e.g., [30–32]).

The long-standing and similar disconnect between field relationships and geobarometric data in the REWP and Snake Range might imply that the story is more complicated, with tectonic overpressure potentially affecting these rocks such that they record pressures greater than lithostatic values (e.g., [33–35]). To explore these issues and provide constraints on the timescales and magnitudes of crustal strain and thickening (Figure 1), we present new field observations derived from detailed geologic mapping, $^{40}Ar/^{39}Ar$ thermochronology, and peak-temperature (T_p) estimates from the least-deformed parts of the REWP core complex in the Pequop Mountains. The Ruby Mountains and East Humboldt Range to the west consist of the same, or slightly lower, stratigraphic units as the Pequop Mountains, but the Ruby Mountains and East Humboldt Range have been pervasively intruded by Mesozoic-Cenozoic intrusions (e.g., [36, 37]) and much of the region was mylonitized during exhumation of these rocks [38]. These features make fundamental field relationships ambiguous, and therefore, we contend that the less deformed and intruded geology in the Pequop Mountains can provide important insights into the tectonic history of the broader REWP region. Deep burial models make specific predictions for the paleo-geothermal structure during peak burial, and our coupled thermochronology-T_p dataset provides a robust test of these hypotheses. We explore the implications of the new data for the development of the Nevadaplano and for the general construction history of orogenic plateaus.

2. Geologic Framework

The REWP core complex [39–42] consists of several north-trending ranges in northeast Nevada (Figure 2(a)) that share similar rock types and tectonic histories. These ranges include, from west to east, respectively, the Ruby Mountains, East Humboldt Range, Wood Hills, and Pequop Mountains (Figure 2). Restoration of Cenozoic extension juxtaposes the constituent REWP ranges [43], demonstrating their geologic connectivity (Figure 2(b)). This restoration is an oversimplification, but most estimates of Cenozoic extension across eastern Nevada suggest at least 50% extension and locally >100% [43, 44], which supports the general pre-Cenozoic framework presented in Figure 2(b). The REWP core complex (Figure 2) exposes variably deformed North American basement and the Neoproterozoic-Triassic passive margin sequence [45, 46], with metamorphic grade generally increasing from east to west, reaching upper amphibolite-granulite facies in the Ruby Mountains [25, 40, 47, 48].

Together, the REWP ranges comprise the footwall of a west-directed detachment-fault system that exhumed rocks either starting in the Late Cretaceous [30] or after 40 Ma [49]. Peak-pressure estimates from the lower part of the Neoproterozoic-Triassic stratigraphy across the REWP are ~6–10 kbar at temperatures of 500-700°C [23, 25, 48, 50],

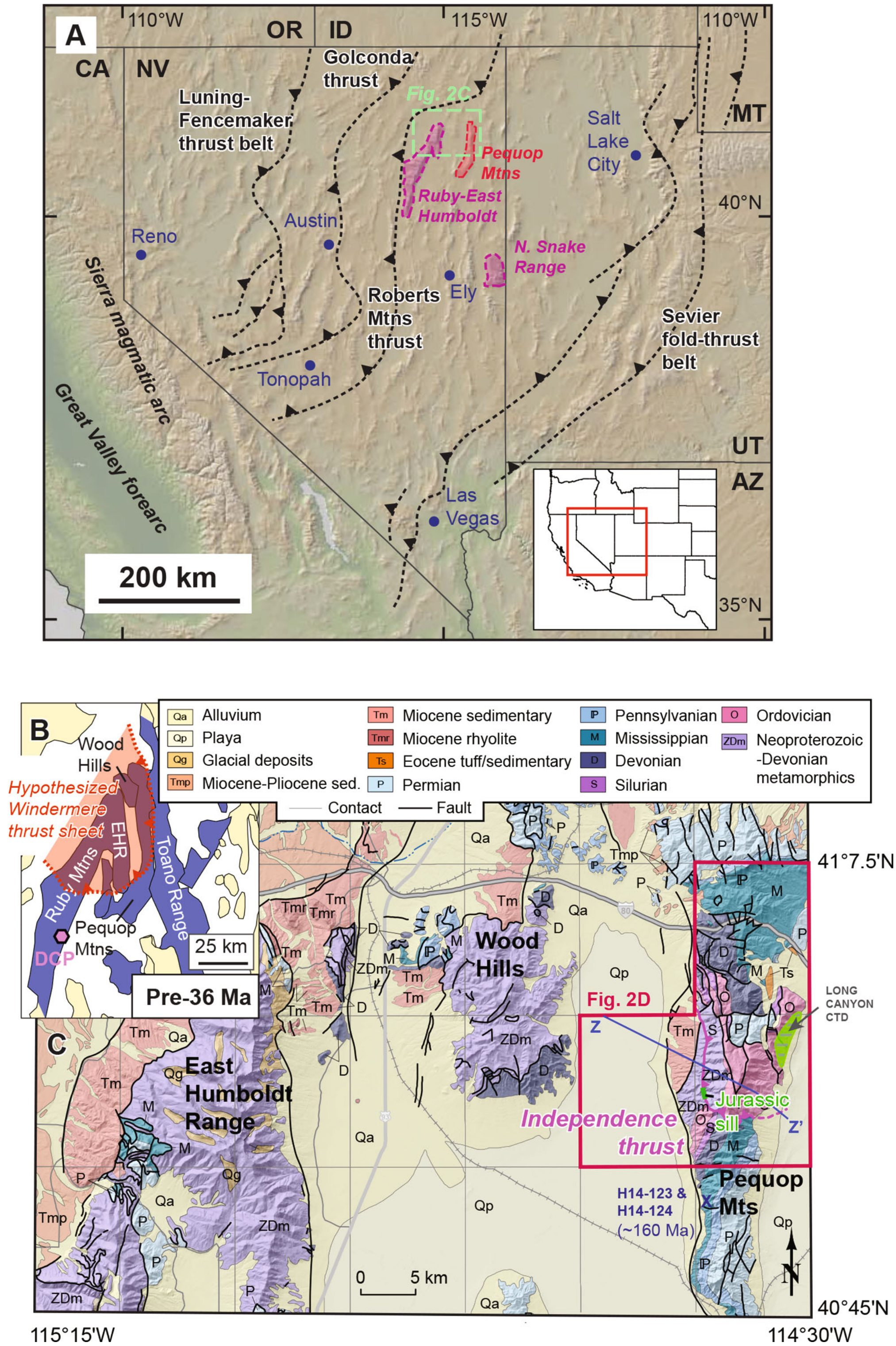

Figure 2: Continued.

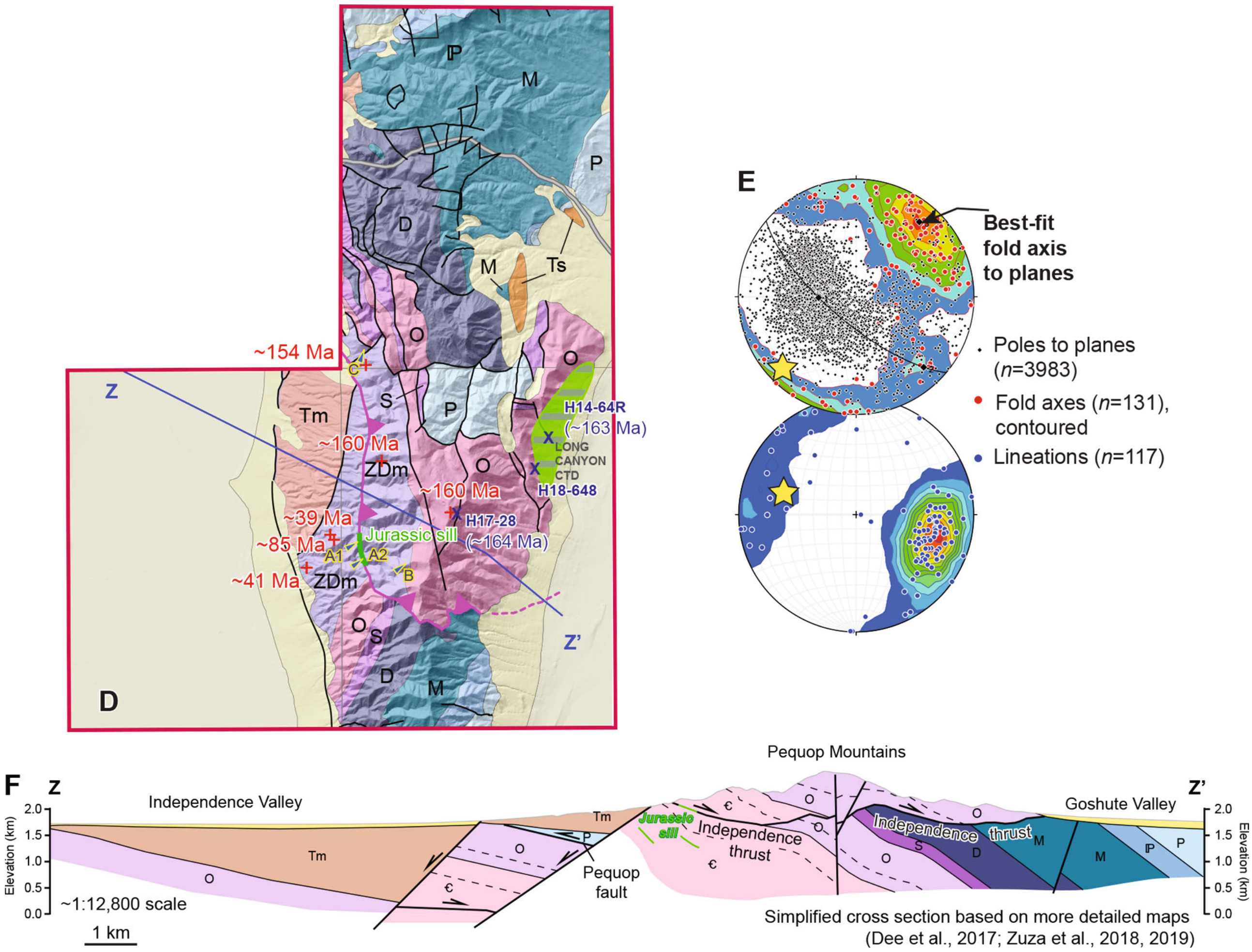

Figure 2: (a) Regional map of the Great Basin schematically showing major Paleozoic-Mesozoic thrust systems [16, 26]. Also shown are the locations of the Ruby Mountains-East Humboldt-Wood Hills-Pequop (REWP) and northern Snake Range core complexes in purple and Pequop Mountains in red. Dashed green box shows approximate location of (c). Inset with red locator box shows the location of (a) in the context of the western United States. AZ: Arizona; CA: California; ID: Idaho; NV: Nevada; OR: Oregon; UT: Utah. (b) Simplified restoration of ranges prior to Cenozoic extension [43] with fault trace of hypothesized Windermere thrust. EHR: East Humboldt Range; DCP: Dawley Canyon pluton. (c) Geologic map of the Ruby Mountains-East Humboldt Range-Wood Hills-Pequop core complex [168] and modified by our new mapping in red box (d). The location of both samples H14-123 and H14-124 dated in this study, just outside of the red box map area, is shown. (d) Zoomed in map of (c) showing the northern Pequop Mountains, including the locations of field photos shown in Figure 4 (blue and yellow triangles, letter/number corresponds to panel). Locations of samples dated in this study shown in blue, and compiled igneous ages from the northern Pequop Mountains shown with red crosses (sources in Table 1). (e) Stereonets of field observations consistent with dominant NW-SE contraction. Star shows location of contour maxima after rotating entire range 40° west, restoring estimated Miocene-to-present tilting [49]. (f) Simplified cross section along Z-Z' (in (c)). Note that the section is at a different scale than (c) and is based on more detailed geologic mapping of Dee et al. [169] and Zuza et al. [68, 83].

suggesting paleo-geothermal gradients of 20–25°C/km. Because the overlying stratigraphic section is ≤10–12 km thick ([47, 51]; Supplemental Figure 1), these estimates suggest >2–3× structural thickening. This may have resulted from the emplacement of the inferred east-directed Windermere thrust sheet [30]. If this model is correct, the thrust's surface expression was obscured or eliminated by later extension.

Most contractional structures in the REWP have been assumed to be Late Cretaceous on the basis of prograde metamorphic ages [50], voluminous Late Cretaceous leucogranites interpreted as crustal melts due to crustal thickening [25, 36, 37, 52], metamorphic zircon rims [53], ca. 83 Ma Lu-Hf garnet ages from the Wood Hills [54], and coeval shortening in the Sevier fold-thrust belt to the east [55, 56]. However, there is also limited evidence for a previous phase of Middle-Late Jurassic deformation recorded in the central Ruby Mountains from metamorphosed xenoliths within the ca. 153 Ma Dawley Canyon pluton [57, 58] (Figure 2(b)). Middle-Late Jurassic deformation has been reported in various ranges throughout eastern Nevada and western Utah (e.g., [59–62]), and this phase of deformation has been referred to as the Elko Orogeny [32, 63]. This region experienced a polyphase history of Mesozoic-Cenozoic intrusion, metamorphism, and deformation, and therefore, the exact age of contractional structures within a particular range can be ambiguous without direct crosscutting relationships.

The Pequop Mountains are the least-deformed part of the REWP core complex and thus provide some of the clearest field relationships, as mentioned previously. The north-trending >80 km long Pequop Mountains span from approximately 41°7.5′N southward to 40°30′N. In this study, our field observations are primarily from the northern Pequop Mountains (e.g., [47]; Figure 2). Early pioneering geologic mapping was completed by Thorman [64, 65] and later by Camilleri [47, 66]. The east-tilted range consists of Neoproterozoic-Triassic strata (Supplemental Figure 1; Supplemental Table 1) that are variably metamorphosed, foliated, and deformed. In general, rocks are most strongly metamorphosed and foliated in the deeper stratigraphic exposures in the west and are minimally deformed in higher stratigraphic exposures in the east (Figure 2). The Independence thrust is the largest observed contractional structure in the Pequop Mountains and has been interpreted to postdate the inferred Windermere thrust ([30]; cf. [67]) (Figure 2). The Independence thrust duplicates ~2 km of stratigraphy, generally placing lower Paleozoic rocks over middle Paleozoic strata. The thrust ramps stratigraphically upsection to the east where Ordovician strata are juxtaposed against Mississippian rocks (Figure 2) [30, 68].

The northern Pequop Mountains have been the focus of recent investigations because of the gold discovery at the Long Canyon Carlin-type gold deposit (CTD) on the eastern flank of the range (Figure 2(c)) (e.g., [69–71]). Jurassic, Cretaceous, and Eocene igneous rocks in the Pequop Mountains have been well characterized and dated by a variety of workers [30, 68–74]. These intrusions are distributed across the range and may link with larger intrusions at depth, which together are thought to have provided the heat source for the Long Canyon mineralization, probably in the Eocene (e.g., [69, 71]).

Table 1 is a compilation of known igneous ages across the range, including three new $^{40}Ar/^{39}Ar$ ages obtained in this study. Jurassic intrusions are either granitic or lamprophyre, including coarsely crystalline equivalent gabbro. Henry and Thorman [74] reported two ca. 160 Ma hornblende $^{40}Ar/^{39}Ar$ plateau ages from lamprophyre from the southern part of the northern Pequop Mountains and several other samples with disturbed spectra indicating either excess Ar or later, probable Cretaceous, reheating. Bedell et al. [69] obtained a mean laser ablation inductively coupled plasma mass spectrometry (LA ICP-MS) $^{206}U/^{238}Pb$ age of ca. 159 Ma but on only two zircon grains from a gabbro in the central Pequop Mountains. A hornblende $^{40}Ar/^{39}Ar$ isochron age of ca. 161 Ma from an unaltered lamprophyre sample collected from the Long Canyon mine was reported by Henry and Thorman [74] (sample H14-64). In this study, we redated this sample (labelled sample H14-64R), as discussed in $^{40}Ar/^{39}Ar$ Thermochronology. Camilleri and Chamberlain [30] documented a boudinaged granitic sill in the western Pequop Mountains and obtained a U-Pb thermal ionization mass spectrometry (TIMS) lower intercept age of ca. 154 Ma defined by five discordant zircon aliquots. Bedell et al. [69] obtained a ca. 160 Ma LA ICP-MS $^{206}U/^{238}Pb$ age on another granitic body ($n = 30$). In summary, all dated lamprophyre intrusions in the Pequop Mountains, and more broadly in northeast Nevada [75–77], are Jurassic in age at ca. 155–160 Ma. That said, Eocene-Oligocene mafic intrusions, mostly gabbro and quartz diorite, in the Ruby Mountains-East Humboldt Range are geochemically similar to the lamprophyres [38, 78–80]. However, the Cenozoic mafic rocks are petrologically and mineralogically dissimilar from northeast Nevada lamprophyres, including those found in the Pequop Mountains. The lamprophyres have biotite or hornblende (±pyroxene) phenocrysts and lack feldspar phenocrysts, whereas the mafic intrusions in the Ruby Mountains-East Humboldt Range contain abundant feldspar phenocrysts [79, 81, 82].

3. Methods and New Data

To investigate deep crustal burial in the REWP core complex by the hypothesized Windermere thrust and to provide age constraints on the timing of contractional deformation in the Pequop Mountains, we (1) documented new field observations that provide age constraints on the Independence thrust and broader regional deformation based on crosscutting relationships; (2) conducted new $^{40}Ar/^{39}Ar$ dating of three mafic intrusions in the Pequop Mountains to integrate with other published data; and (3) examined the thermal structure of the upper crust by compiling existing, and generating new, T_p estimates from multiple methods.

3.1. Field Relationships. We recently completed new geologic mapping of three 7.5′ quadrangles at 1 : 24,000 scale across the northern Pequop Mountains [68, 74, 83] (red box in Figures 2(c) and 2(d)). Neoproterozoic-Triassic bedding and tectonic foliation in the Pequop Mountains primarily dip east-northeast. The only constraints on eastward tilting of the range, which we attribute to Cenozoic extension, are from the 41–39 Ma Nanny Creek volcanic section [72, 73], located just south of Interstate 80 in the Pequop Mountains (unit Ts in Figures 2(c) and 2(d)), which presently dips ~40° east based on the dip of a sedimentary unit within the section [49, 72, 74, 84]. Assuming that the Nanny Creek volcanic and sedimentary rocks were deposited subhorizontally, this implies ~40° eastward tilting of the Pequop Mountains since ca. 39 Ma. We acknowledge that the volcanic rocks could have been deposited with significant primary dips within the paleovalley, complicating the tilt calculation [85]. However, we consider the ~40° east dips measured from a sedimentary unit in the thalweg of this paleovalley [49] to be a close approximation of Nanny Creek paleovalley tilting. We attribute this post 39 Ma tilting primarily to Basin and Range extension accommodated along high-angle normal faults on the western flank of the range that have total normal-sense displacements of 6–7 km based on our geologic mapping and well data (Figure 2(f); [68, 83]), which is consistent with 40° of eastward tilting of the range.

Table 1: $^{40}Ar/^{39}Ar$ and U-Pb ages of pre-Cenozoic intrusions, Pequop Mountains, Nevada.

Sample	Rock type	Location	Materials	Age (Ma)[1]									Latitude	Longitude	Source
$^{40}Ar/^{39}Ar$ analyses (step heating)				Plateau	±2σ	%^{39}Ar[3]	Steps[2]	Isochron	±2σ	MSWD	Total gas	±2σ			
H14-88	Muscovite leucogranite	South Pequop	Muscovite	NM				85.1	0.2		78.4	0.2	40.94280	-114.62859	[74]
H14-123	Lamprophyre	South Pequop	Hornblende	161.5	0.2	74.8	3/7	158	3	14	160.3	0.1	40.84993	-114.61219	[74]
H14-124	Lamprophyre	South Pequop	Hornblende	159.6	0.2	53.7	3/15	159.1	0.6	0.16	155.4	0.1	40.84993	-114.61219	[74]
H17-28	Gabbro	Central Pequop	Hornblende	164.1	1.3	75.5	5/10	159.6	2.0	0.7	174.6	0.5	40.94148	-114.57769	This study
H14-64	Lamprophyre	Long Canyon	Hornblende	Excess Ar				160.9	0.5	453	166.6	0.5	40.97257	-114.52677	[74]
H09-93B	Lamprophyre	Long Canyon	Hornblende	Excess Ar				165	2	186	209	1.0	40.97163	114.52669	[74]
CLC-207	Lamprophyre	Long Canyon	Biotite	Highly disturbed, probably Jurassic				127	9	10000	147	0.1	40.98360	-114.52340	[74]
MRLC-1	Lamprophyre	Long Canyon	Biotite	Highly disturbed, probably Jurassic				132	5	200	138	0.1	40.96640	-114.53500	[74]
H18-648	Lamprophyre	Long Canyon	Biotite	Highly disturbed, probably Jurassic				140	1	83	136	0.7	40.96591	-114.53629	This study
H14-64R	Lamprophyre	Long Canyon	Hornblende	163.2	1.5	51.5	7/10	157.0	4.0	3.6	183.5	1.0	40.97257	-114.52677	This study
U-Pb zircon analyses				Low intercept	±1σ	n^2	$^{206}Pb/^{238}U$	±1σ			Upper intercept				
151P	Foliated granitic dike	West Pequop	TIMS	154	5						~2400		40.9942	-114.6125	[30]
PQSG	Gabbro	Central Pequop	LA-ICPMS			2	159.0	6.0					40.9417	-114.5789	[69]
34FGG	Foliated rhyolite dike	West Pequop	LA-ICPMS			14	159.5	1.9					40.9635	-114.6048	[69]
SWPQR1	Rhyolite dike	Southwest Pequop	LA-ICPMS			6	41.0	0.8					40.9299	-114.6427	[69]
SWPQR2	Rhyolite dike	Southwest Pequop	LA-ICPMS			12	39.1	0.7					40.9433	-114.6296	[69]
SWCGG	Leucogranite dike	Southwest Pequop	LA-ICPMS			2	71.0	5.0					40.9396	-144.6324	[69]
Rockland	Granodiorite	South Pequop	LA-ICPMS				161.4	1.9					40.7914	-114.6194	[69]

(1) $^{40}Ar/^{39}Ar$ analyses of this study were at the New Mexico Geochronological Research Laboratory (methodology in [86]). Neutron flux monitor fish canyon tuff sanidine (FC-1) with assigned age = 28.201 Ma [88]. Published ages of Brooks et al. [72, 73] were recalculated to the same monitor age. Decay constants after Min et al. [170]; $\lambda_{total} = 5.463 \times 10^{-10}\ yr^{-1}$. Isotopic abundances after Steiger and Jager [171]; $^{40}K/K = 1.167 \times 10^{-4}$. (2) n or steps = number of steps used in age calculation/total number of analytical steps. (3) %^{39}Ar = percentage of ^{39}Ar used to defined plateau age. NM = not meaningful; no plateau.

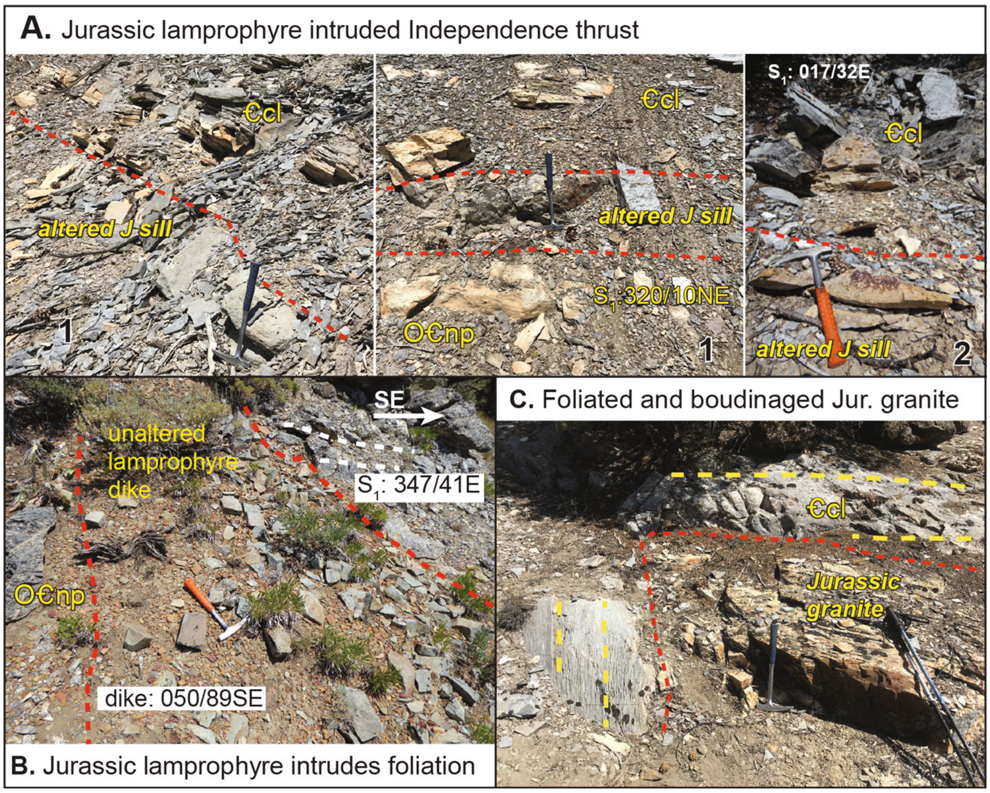

FIGURE 3: Field photographs of important crosscutting relationships in the Pequop Mountains, with locations shown in Figure 2. (a) Jurassic lamprophyre intruded into the Independence thrust, where it places Cambrian Cliffside Limestone (Єcl) over Cambrian-Ordovician Notch Peak Dolomite (OЄnp). Locations: (1) 114.6176°W, 40.9390°N; (2) 114.6161°W, 40.9347°N (all WGS1984). (b) Unaltered undeformed Jurassic lamprophyre dike crosscuts OЄnp foliation. Location: 114.59564°W, 40.93222°N. (c) Boudinaged Jurassic granite surrounded by Єcl limestone. Note that where the granite pinches out, the surrounding limestone merges. Location: 114.61275°W, 40.99429°N.

Unit contacts on the geologic maps and cross sections (Figure 2) appear to suggest parallel undeformed stratigraphy, but the lower and middle Paleozoic units are variably internally deformed with local boudinage development, bedding-parallel faulting, shearing, thrust faulting, and folding. Deformation is strongly partitioned to the mechanically weaker horizons, such as limestone marbles, with the stronger beds commonly completely undeformed, including quartzite or dolomite (e.g., [68, 71]). Competent rocks such as quartzite, dolomite, and granitic rocks are boudinaged with weaker limestone marble flowing around them. Boudinage orientations and stretching lineations both suggest northwest-southeast stretching and contractional shearing (Figure 2(e)). Asymmetric shear fabrics, folds, and minor faults observed throughout the range suggest a top-southeast shear sense (Figure 2(e)). We verified that post-39 Ma tilting of the range, as evidenced by the Nanny Creek volcanic section, does not significantly change the observed southeast-shear direction by retro-deforming the ~40° of eastward tilting on stereonets (star in Figure 2(e)). We acknowledge that the range may have tilted more or less to the north or south, but these are the only tilting constraints available in the Pequop Mountains.

The Independence thrust is poorly exposed on the western side of the range, but is well exposed on the eastern flank where Thorman [65] originally referred to it as the Valley View thrust. Its trace, identified primarily by consistent older-over-younger unit juxtapositions, traverses the Pequop Mountains (Figure 2). This east-southeast-directed fault places lower Paleozoic rocks over middle Paleozoic strata, duplicating ~2 km of stratigraphy (Figure 2). Metamorphic foliations, which are generally parallel to unit contacts, generally become subparallel to the thrust within ~50m structural distance. Near the fault, rocks are highly strained, commonly exhibiting southeast-trending lineations and southeast-vergent folds and shear fabrics.

In two localities along the western flank of the northern Pequop Mountains, we observed lamprophyre sills that intruded the Independence thrust [68] (Figure 3(a)). The sills are weakly foliated and altered. The sills at both locations yielded no zircon, but as previously mentioned, all known lamprophyre intrusions across the Pequop Mountains, and more broadly in northeast Nevada, are Jurassic in age at ca. 155–160 Ma (Table 1). We expand on this point below in Discussion. This thrust-intruded sill provides a critical age relationship for the Independence thrust, such that the thrust must have been active prior to the lamprophyre intrusion. The timing of weak foliation development is unconstrained: it may have occurred shortly after intrusion or during a later Late Cretaceous event. Other crosscutting relationships across the northern Pequop Mountains include syn-to-post-kinematic Jurassic intrusions in foliated Cambrian strata (Figure 3(b)) and a boudinaged Jurassic granite with Cambrian limestone flowing around it (Figure 3(c)) (e.g., [70]).

3.2. $^{40}Ar/^{39}Ar$ Thermochronology. Minerals from three mafic rocks were analyzed via ^{40}Ar/^{39}Ar thermochronology, including two lamprophyre dikes collected from the Long Canyon mine area on the eastern flank of the Pequop Mountains and one gabbro intrusion—a coarsely crystalline lamprophyre—collected from the central ridge of the Pequop Mountains (Table 1). We also discuss two lamprophyre ages presented previously in Henry and Thorman [74]. Hornblende and/or biotite were separated from the samples following standard mineral separation techniques at the University of Nevada, Reno. Samples were irradiated at the TRIGA reactor at Oregon State University and analyzed at the New Mexico Geochronology Research Laboratory at the New Mexico Institute of Mining and Technology using procedures described in McIntosh et al. [86] and Henry et al. [87]. Neutron flux was monitored using Fish Canyon Tuff sanidine (FC – 1 = 28.201 Ma; [88]). Complete analytical data are presented in Supplemental Table 2 and age spectra are shown in Figure 4.

Hornblende from lamprophyre sample H14-64R yielded a plateau age of 163.2 ± 1.4 Ma (MSWD: 1.54) and an isochron age of 157.0 ± 4.0 Ma, and hornblende from gabbro sample H17-28 yielded a plateau age of 164.1 ± 1.3 Ma (MSWD: 8.15) and an isochron age of 159.6 ± 2.0 Ma (Figure 4; Table 1). Given the high effective closure temperature of Ar in hornblende (i.e., 500–550°C), depending on cooling rate and grain properties [89, 90], we interpret Late Middle Jurassic ages to record conductive cooling shortly after intrusion. These ages demonstrate that the samples were not subsequently heated to temperatures > 500°C since ca. 160 Ma. Samples H14-123 and H14-124 were both collected from the same lamprophyre sill outcrop in the southern part of the northern Pequop Mountains (Figure 2(d)), and they yielded well-defined plateau ages of 161.5 ± 0.2 Ma (MSWD: 14.28) and 159.6 ± 0.2 Ma (MSWD: 1.96) (Figure 4; Table 1; [74]), respectively. We also interpret these ca. 160 Ma ages as representing a time near original intrusion.

Biotite from lamprophyre sample H18-648, collected near Long Canyon, yielded a disturbed spectrum with no plateau (Figure 4). Several steps have ca. 160 Ma ages, but most are 130–140 Ma. We interpret that this sample recorded some component of Late Jurassic cooling that was subsequently disturbed, possibly due to partial reheating or fluid alteration. This sample (H18-648) was collected from the same region within Long Canyon as sample H14-64R, and we would expect the same thermal history to have affected both samples. The closure temperature of Ar diffusion in biotite (i.e., 250–350°C; e.g., [91]) is lower than that of hornblende, and thus, sample H18-648 may be recording partial reheating at temperatures approaching 300°C. Evidence to support the interpretation that heat and/or fluids affected sample H18-648 include (1) significant alteration around Long Canyon and throughout the Pequop Mountains, including decarbonization, argillic alteration, silicification, and dolomitization [71], (2) hornfelsic textures in some of the shaley units such as the Mississippian Chainman Shale, and (3) sugary cryptocrystalline textures observed during our conodont color alteration index (CAI) analyses that are interpreted to represent alteration by hydrothermal fluids, as discussed in more detail below.

3.3. Peak Temperature Estimates. Existing published peak temperature estimates from across the Pequop Mountains consist of calcite-dolomite thermometry [92], Raman spectroscopy of carbonaceous material (RSCM) ([92]; this study), and semiquantitative deformation temperature ranges from dynamic quartz recrystallization microstructures [93]. We conducted new RSCM and conodont color alteration index (CAI) analyses to supplement published data. RSCM thermometry was conducted following methods outlined in Cooper et al. [94] and Long and Soignard [95]. During progressive heating and solid-state metamorphism, carbonaceous material in a rock transforms to graphite, and the RSCM procedure is based on the temperature dependence of the degree of structural organization of graphite bonds. Therefore, this structural organization can be used as a thermometer (e.g., [94, 96–98]). The height ratio (R1) and area ratio (R2) of four first-order Raman spectrum peaks (G, D1, D2, D3) in the wavenumber offset range between 1200 cm^{-1} and 1800 cm^{-1} were used in conjunction with Equations 1, 2, and 3, of the Rahl et al. [98] calibration to determine peak temperatures. This results in typical uncertainties of ~30–50°C over the peak temperature range of 100°C to 700°C.

Carbonaceous material was analyzed *in situ* on polished thin sections (Figure 5). Analyses were conducted on a Raman spectrometer at the LeRoy Eyring Center for Solid State Science at Arizona State University. The 532 nm laser was operated at a power of 3 mW and was focused using a 50× ultralong working distance Mitutoyo objective. Instrument parameters, settings, and procedures follow those outlined in Cooper et al. [94]. Carbonaceous material was analyzed for 120 seconds over a spectral window of 1100-1800 cm^{-1}, and typically, 15 separate spots were analyzed in each sample. The peak positions, heights, widths, and areas of the Raman spectra were determined using a custom Matlab peak fitting program written by E. Soignard, which allowed peak shapes to be fit by a combination of Gaussian and Lorentzian peaks. Any background slope was removed by using a first-order polynomial between 1100 cm^{-1} and 1800 cm^{-1}. Examples of representative Raman spectra for each sample are shown in Figure 5(f). Table 2 presents a summary of mean R1 and R2 values and peak temperature determinations, and the complete information for all analyses are provided in Supplemental Table 3.

Conodonts are the phosphatic teeth of a nektonic eel-like chordate that inhabited all marine settings from Cambrian to Triassic time. In this study, they were recovered from dissolution of carbonate samples in 10% formic acid. The color alteration index for organic metamorphism of conodonts was developed by Anita G. Harris and first published in Epstein et al. [99]. The method is based on empirical evidence that conodonts predictably change color with increasing temperature [99]. CAI values were determined under

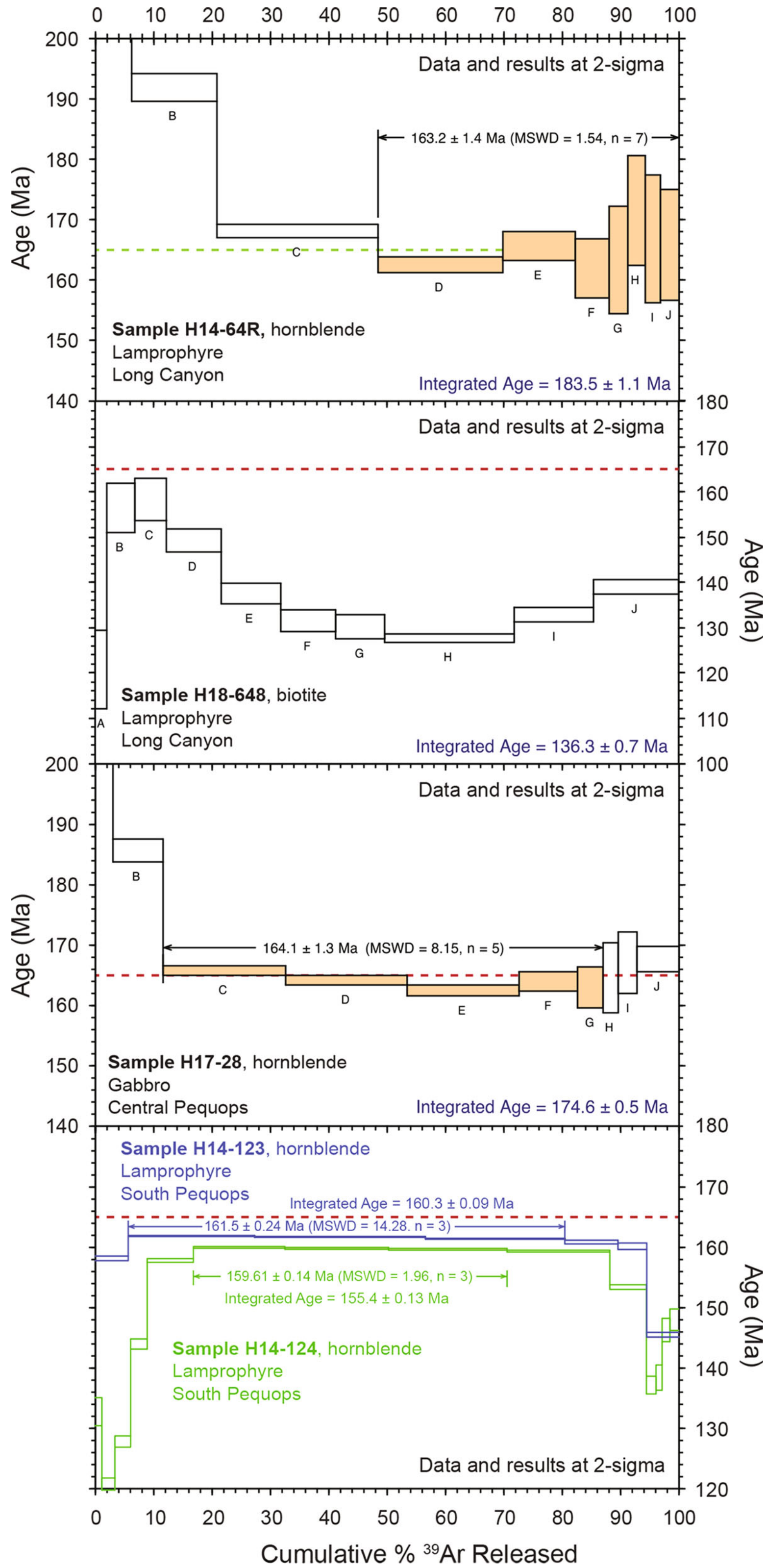

FIGURE 4: $^{40}Ar/^{39}Ar$ step-heating spectra for samples analyzed from the Pequop Mountains in this study and Henry and Thorman [74]. Unfilled steps were not included in the plateau age calculation. Letters correspond to step ID in Supplemental Table 2. Dashed red line at 165 Ma in all panels for comparison. The lowermost part of the image shows two spectra from lamprophyre samples from the southern Pequop Mountains presented in Henry and Thorman [74].

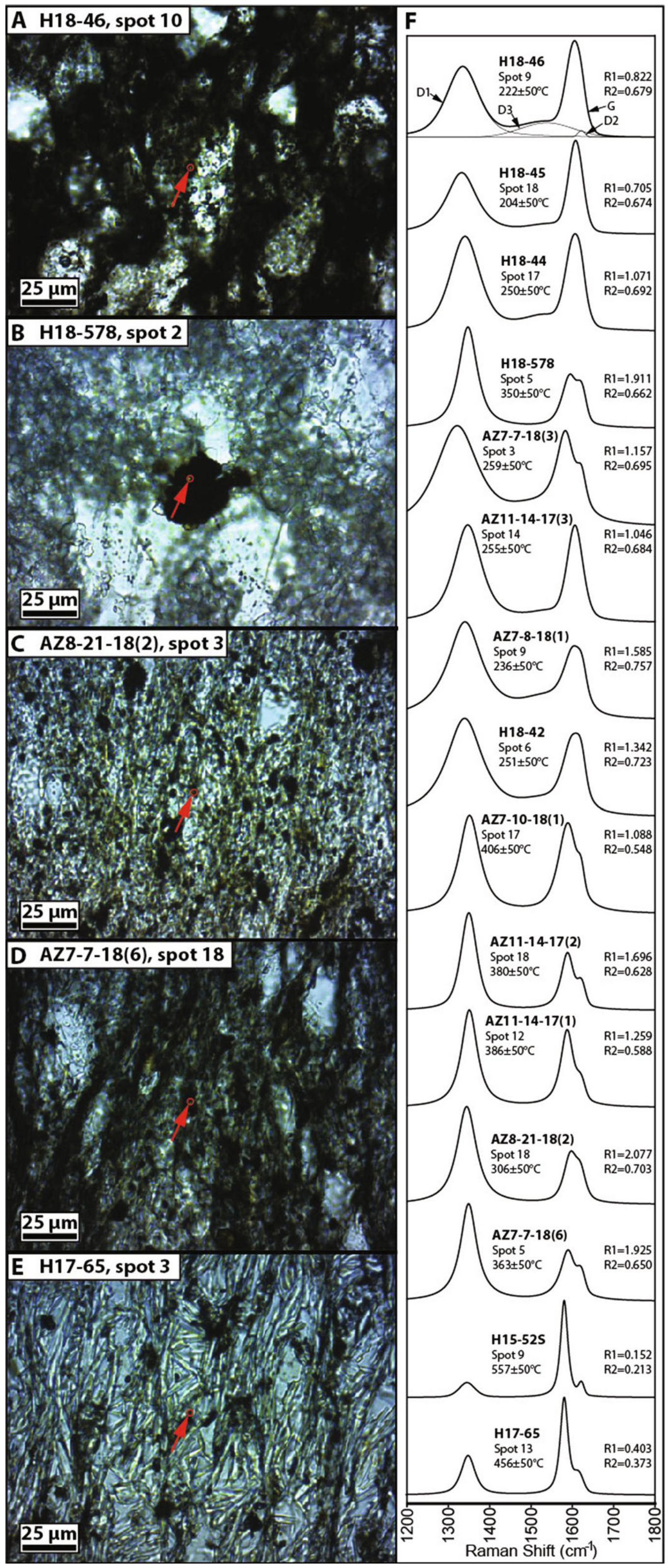

Figure 5: Example photomicrographs and representative Raman spectra from the samples analyzed for Raman spectroscopy on carbonaceous material thermometry. The positions of the graphite band (G) and defect bands (D1, D2, D3) are shown on the top spectrum. Peak temperatures (T) and R1 and R2 parameters are calculated after Rahl et al. [98]. Supplemental Table 3 lists peak center position, height, amplitude, and area for individual analyses.

Table 2: Summary of RSCM analyses on Pequop Mountain samples.

Sample	Map Unit	R1 Mean	R1 1σ	R2 Mean	R2 1σ	Peak temperature (°C) Mean	1σ	2σ	n
H18-46	Pp	0.898	0.129	0.688	0.017	225	16	28	14
H18-45	Pp	0.913	0.116	0.707	0.035	208	29	29	16
H18-44	Pe	1.175	0.158	0.704	0.022	250	27	27	18
H18-578	Pe	1.893	0.229	0.683	0.055	323	66	39	18
AZ7-7-18(3)	Mc	1.189	0.215	0.693	0.052	262	53	39	14
AZ11-14-17(3)	Mc	1.125	0.162	0.692	0.020	255	34	36	11
AZ7-8-18(1)	Mc	1.393	0.116	0.746	0.022	231	23	27	17
H18-42	Mc	1.375	0.083	0.727	0.017	250	20	26	17
AZ7-10-18(1)	Mc	1.190	0.104	0.562	0.024	405	14	28	14
AZ11-14-17(2)	Ds	1.714	0.345	0.620	0.042	379	31	28	17
AZ11-14-17(1)	Ds	1.264	0.223	0.579	0.063	392	52	39	14
AZ8-21-18(2)	Opks	2.205	0.246	0.692	0.036	310	44	37	13
AZ7-7-18(6)	Opks	1.928	0.134	0.650	0.019	361	18	25	18
H15-52S	Cd	0.156	0.010	0.217	0.019	554	18	27	15
H17-65	Cd	0.425	0.072	0.378	0.029	456	21	33	11

Footnote: R1, R2, and peak temperature values calculated using the calibration of Rahl et al. [98]. Internal variability in R1, R2, and peak temperature is indicated by 1σ uncertainty. Temperature is also reported with 2 standard errors (SE), calculated after Cooper et al. [94], from quadratic addition of 1σ internal error and external error of ±50°C from the Rahl et al. [98] calibration, divided by the square root of the number of analyses (*n*).

incident light using the calibrated color chart of Epstein et al. [99], which is calibrated from 50°C to >600°C. Conodonts typically had a lustrous shiny surface, but some had a sugary cryptocrystalline texture that was interpreted to represent hydrothermal alteration; these samples are marked by an asterisk in the data table (Table 3) and a white symbol in Figure 6 plots. CAI values from hydrothermally altered conodonts are still reported, but we emphasize that they record hotter temperatures associated with hydrothermal fluids. To facilitate comparison to other temperature estimates, we converted CAI values to absolute temperatures with relevant uncertainties following the scheme presented in Supplemental Table 4, which was derived from Epstein et al. [99]. Table 3 presents analyzed samples, their locations, their CAI values, and the corresponding converted temperature ranges.

We compiled new and existing T_p from northeast Nevada using data from the following sources: new CAI and RSCM temperature estimates presented in this study, RSCM data from the Pequop Mountains [92], calcite-dolomite temperatures from the Pequop Mountains ([92], with the calibration of [100]), and descriptions of dynamic quartz recrystallization microstructures from the Pequop Mountains from Latham [93] (data tabulated in Supplemental Table 5; Figure 6). We projected T_p onto the Neoproterozoic-Triassic stratigraphy using thicknesses presented in Zuza et al. [68]; cumulative thickness values for each unit are in Supplemental Table 5 (drafted in Supplemental Figure 1). These stratigraphic thicknesses are similar to those of Camilleri [47] and Ketner et al. [101]. Depth versus T_p is plotted in Figure 6(a), with an additional 2 km added to the thickness values to account for structural thickening related to the Independence thrust and parallel contractional folding and minor faulting. Note that removing this 2 km correction does not change our interpretations.

The T_p synthesis reveals that peak temperatures increase with stratigraphic depth. At a given stratigraphic depth, different peak temperature methods reveal broadly similar temperature ranges. However, the RSCM data (this study; Howland [92]) appear systematically ~50–100°C hotter than the calcite-dolomite thermometry temperatures of Howland [92]. There are several possible explanations for this. First, Howland [92] used the calibration of Anovitz and Essene [100]. Herwegh and Pfiffner [102] noted that of the published calibrations, Anovitz and Essene [100] yielded systemically lower temperature estimates (i.e., generally 50–75°C lower) than other available thermometers [103–106]. We do not attempt to recalculate Howland [93] data with another calibration, but note that choosing a different calibration could shift the data to be more compatible with the RSCM results (Figure 6(a)). Second, the two thermometers involve different timescales to equilibrate: graphite bond ordering recorded by RSCM may take only 100 s of years [107], whereas Ca-Mg diffusion for calcite-dolomite thermometry operates on slower timescales of >0.1–1.0 Myr, based on experimentally derived diffusion coefficients for Ca and Mg (e.g., [108, 109]). The RSCM data thus may partially reflect local short timescale thermal pulses that cause the T_p values to be higher than calcite-dolomite thermometry. Depending on the rates of heating, the calcite-dolomite thermometer could record slightly lower temperatures if final peak heating is relatively short-lived (<1 Myr).

Temperatures vary by as much as ~300°C at any given stratigraphic depth (Figure 6(a)), which we interpret resulted from the small-scale intrusions that are distributed across the range that may link with larger intrusive bodies at depth ([69,

Table 3: CAI data from the Pequop Mountains.

Sample	Latitude	Longitude	Unit	CAI	Converted temperature (°C)
P197	41.05054	-114.58216	Mtp	3.5	200 ± 50
P198	41.05050	-114.58200	Mtp	3.5	200 ± 50
P568	41.13469	-114.58767	Pp	1	60 ± 20
P592a	41.00704	-114.55206	Mtp	3.5	200 ± 50
P720	41.07653	-114.59411	Mtp	5.5∗	425 ± 90
P725	40.86675	-114.61242	Dg	4	245 ± 55
P726	40.86569	-114.61775	Dg	4.5	318 ± 70
P782	40.86536	-114.61356	Mtp	5∗	390 ± 90
P784	40.86525	-114.61261	Mc	5	390 ± 90
P828	40.86869	-114.61181	Mtp	7∗	605 ± 115
P829	40.86856	-114.61144	Mtp	5∗	390 ± 90
P890	40.97711	-114.56686	Pe	2.5	128 ± 45
P950	41.04763	-114.61594	Dg	5	390 ± 90
P951	41.03344	-114.62563	Srm	4.5	318 ± 70
P952	41.02333	-114.58848	Srm	4.5	318 ± 70
P953B	41.00740	-114.59177	Opl	4.5	318 ± 70
P967	40.97917	-114.56573	Pe	4.5	318 ± 70
P989	40.87710	-114.61930	Dg	5	390 ± 90
P991	41.11948	-114.57990	Pe	2.5	128 ± 45
P992	41.14418	-114.60635	Pp	1.5	70 ± 20
P1010	40.89175	-114.56029	Pe	1	60 ± 20
P1013	41.00128	-114.59484	Opkl	5	390 ± 90
P1085	40.86683	-114.61227	Dg	5.5-6∗	425 ± 90
P1086	40.86693	-114.61227	Mtp	5.5-6∗	425 ± 90

∗Cryptocrystalline texture suggesting hydrothermal alteration; used lower CAI value if range is given.

71]; Figure 2; Table 1). However, assuming that the coldest samples at a given depth best represent the regional thermal gradient, the data show a relatively high geothermal gradient of ~40–50°C/km. High thermal gradients are similar to other estimates in the eastern Great Basin [21, 44, 92, 110, 111] and confirm the importance of intrusions affecting the thermal structure of the crust. Recent $^{40}Ar/^{39}Ar$ thermochronology, including mica and potassium feldspar analyses, suggests that these high geothermal gradients probably existed in the Late Cretaceous and Eocene [83].

4. Discussion

4.1. Jurassic Contractional Deformation in the Pequop Mountains. Most of the structural features observed in the Pequop Mountains are consistent with top-southeast shearing (Figure 2). This includes subparallel foliations, northwest-southeast trending lineations, and a top-southeast shear sense observed for the intraformational folds and faults and the larger Independence thrust (Figure 2). The simplest interpretation is that all of this deformation was contemporaneous. The intraformational shear fabrics and boudinage structures suggest transport-parallel lengthening during motion on the Independence thrust (i.e., top-southeast), which is consistent with nonrigid wallrock deformation [112] during regional thrust transport as commonly observed in Himalayan shear zones (e.g., [95, 113]).

The timing of this deformation is bracketed by crosscutting field relationships. As already outlined, both sheared foliations and the Independence thrust were intruded by undeformed or synkinematic dikes and sills. The lamprophyre sill that intruded the Independence thrust in two locations (Figure 3(a)) is not dated directly. The sill yielded no zircon and is too altered for other chronology methods. However, as summarized in Table 1, all dated lamprophyre intrusions in northeast Nevada are Jurassic in age at ca. 155–160 Ma [75–77], including new ages from this study (Figure 4). The geochemical characteristics of the Jurassic intrusions are readily distinguishable from other local Jurassic, Cretaceous, and Eocene intrusions. Jurassic lamprophyres and other related mafic intrusions have lower silica content ($SiO_2 < 50\%$ to ~60%) and higher titanium ($TiO_2 > 1\%$) than Jurassic rhyolites, Eocene rhyolites, or Cretaceous (?) leucogranites (complete data table in [68]) (Figure 7(a)). Rare-earth element concentrations from Cretaceous leucogranites are also significantly lower than any of the lamprophyres, and Ta concentrations in the Cretaceous leucogranites are much higher (Ta > 20 ppm) (Figure 7(b)). Eocene quartz diorites in the East Humboldt Range are geochemically similar to the Jurassic Pequop Mountains lamprophyres, except the lamprophyres have significantly higher V (Figure 7(c)), plotted using unpublished data from A. J. McGrew reported in the du Bray et al. [114] database. As previously mentioned, the Jurassic lamprophyres are also petrologically and mineralogically dissimilar from Eocene quartz diorite because the lamprophyres are distinctive with biotite or hornblende (±pyroxene) phenocrysts and no feldspar phenocrysts, whereas the Eocene mafic intrusions in the Ruby Mountains-East Humboldt Range have feldspar phenocrysts [79, 81, 82].

Accordingly, we argue that the undated lamprophyre sill that intruded the Independence thrust is Late Jurassic in age, similar to all other lamprophyre sills in the region. Other syn-to-post kinematic intrusions in the Pequop Mountains crosscut foliated Cambrian strata (Figure 3(b)) and a Jurassic granite is boudinaged with Cambrian limestone flowing around it (Figure 3(c)) (e.g., [70]). In the Toano Range, the next range to the east of the Pequop Mountains (Figure 2(b)), foliated and deformed lower Paleozoic rocks are crosscut by the undeformed Jurassic Silver Zone Pass granodiorite pluton [101] and lamprophyre dikes in the contact aureole. The Silver Zone Pass yielded U-Pb zircon ages of 162 Ma (J. E. Wright personal communication, 1986, cited in [115]) and 157 Ma [116]. The ca. 153 Ma Dawley Canyon pluton in the central Ruby Mountains (Figure 2(b)) was interpreted to be synkinematic with respect to amphibolite-facies metamorphism and deformation [57, 58].

In summary, field observations suggest that the contractional structures observed across the northern Pequop

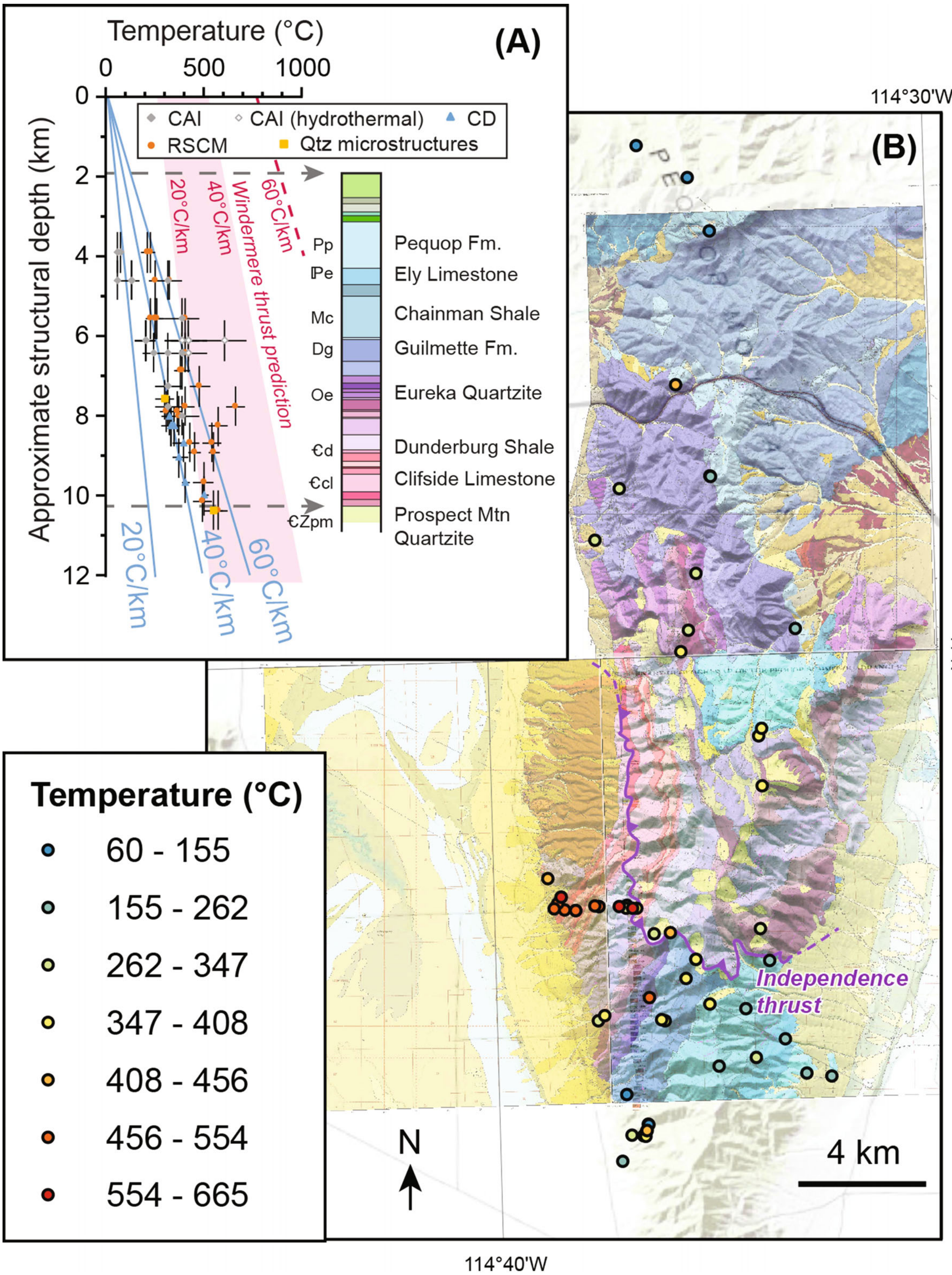

Figure 6: (a) Stratigraphic depth (0.5 km uncertainty) versus T_p across the Pequop Mountains, with sample locations shown in (b). Note that ~2 km thickening is invoked based on mapped Independence thrust relationships; see text. Accompanying stratigraphic column (same vertical scale) shows observed thicknesses [68]. Only some units are named; the complete stratigraphic column is in the Supporting Information. Data: CAI (this study); RSCM (this study; [92]); calcite-dolomite thermometry (CD) [92]; quartz recrystallization microstructures [93]. CAI data with white symbol and brown outline are interpreted to have been affected by hydrothermal fluids. Predicted thermal structure assuming Windermere thrust hypothesis is shown in red. (b) Map showing locations of T_p samples plotted in (a), colored by peak temperature, plotted on three new published quadrangle maps [68, 74, 83]. At this scale, the maps are not entirely legible, but readers are referred to Figure 2 or the map references.

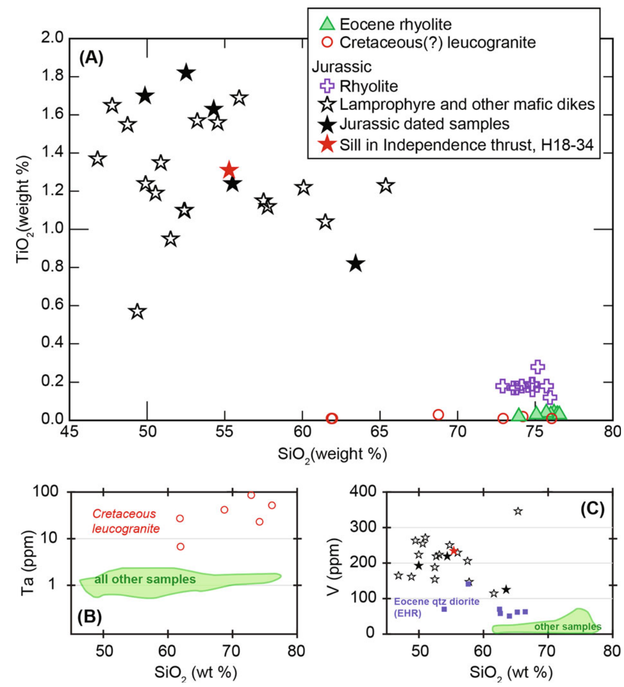

Figure 7: (a) SiO_2 versus TiO_2 (weight %) of intrusions in the Pequop Mountains demonstrating the similarity of Jurassic lamprophyre intrusions and their uniqueness relative to Eocene rhyolite, Cretaceous rhyolite, and Jurassic rhyolite (data from [68]). Red star indicates the sample collected from the lamprophyre sill that intruded the Independence thrust; the sample is similar to dated Jurassic lamprophyre intrusions. (b) SiO_2 (weight %) versus Ta (ppm), highlighting how the Cretaceous leucogranites are distinct from the other igneous rocks (green envelope) in the northern Pequop Mountains. (c) SiO_2 (weight %) versus V (ppm), including data from Eocene quartz diorite rocks of the East Humboldt Range (EHR) (A. J. McGrew unpublished data compiled from [114] database), showing how Jurassic lamprophyre intrusions are geochemically distinct from these mafic rocks in the EHR.

Mountains developed in the Late Jurassic at ca. 160 Ma or just immediately prior. Jurassic contractional deformation is reported elsewhere in eastern Nevada (e.g., [61]) and comprises the Elko Orogeny of Thorman et al. [32].

4.2. Limited Structural Thickening. Field relationships and T_p from the Pequop Mountains are inconsistent with deep burial [117] by the hypothesized Windermere thrust sheet. Continuous stratigraphy across the range transitions from Neoproterozoic-Cambrian rocks on the western flank to undeformed Permian strata on the eastern flank with no structural break [47, 68] (Figures 2(b) and 2(c)) at a latitude of approximately 40°51′N. Stratigraphic depth versus T_p similarly shows a monotonic increase of temperature with depth, consistent with a relatively high geothermal gradient of ~40–50°C/km (Figure 6). The apparent negative y-intercept of these correlations (depths > 2 km) at $T_p = 0°C$ is inconsistent with any burial by the Windermere thrust sheet. If these rocks were buried by a ~15 km thick thrust sheet, an improbably low <5 C°/km gradient would be required, which is inconsistent with other estimates of paleo-geothermal gradients in the region (e.g., [21, 92, 110, 111, 118]) and the modern Great Basin thermal structure [119, 120]. Also, CAI values of 1 to 2 in the Pennsylvanian and Permian strata (Table 3) preclude such a burial depth. Therefore, the T_p data are best interpreted as a high thermal gradient through Neoproterozoic-Triassic stratigraphy that was never buried beyond original stratigraphic depths.

In addition, Windermere thrust geometries are difficult to reconcile. Camilleri and Chamberlain [30] speculated that the east-directed thrust emerged between the Pequop and Toano ranges, which were adjacent prior to extension (Figure 2(b)). The geology across both ranges is similar, including metamorphosed lower Paleozoic strata crosscut by Jurassic intrusions [61, 101]. South of ~40.4°N, strata in the Pequop and Ruby Mountains show no signs of significant burial [51, 121], and regional compilations of erosion levels beneath Cenozoic rocks reveal no trace of this structure, or comparable structures, anywhere to the south [122–125]. The Windermere thrust sheet would have been >15 km thick, ~50 km wide (N-S direction), and overthrust the REWP with a transport-parallel distance of 70+ km. This geometry is entirely atypical of contractional structures in eastern Nevada (e.g., [21, 52, 126]) and dissimilar to typical thrust sheets mapped or geophysically imaged in other hinterland regions, such as in Tibet and the Andes (e.g., [83, 127–132]). In summary, the lack of field evidence, our refined Jurassic age for the Independence thrust, and T_p data from the Pequop Mountains all make the Cretaceous Windermere thrust hypothesis insubstantial.

4.3. Deformation in the Cordilleran Hinterland and Growth of the Nevadaplano. Jurassic strain in the Pequop Mountains can be placed in the larger spatial framework of other Jurassic structures in the eastern Great Basin [32, 59, 61, 63], which temporally overlaps with the Luning-Fencemaker thrust belt

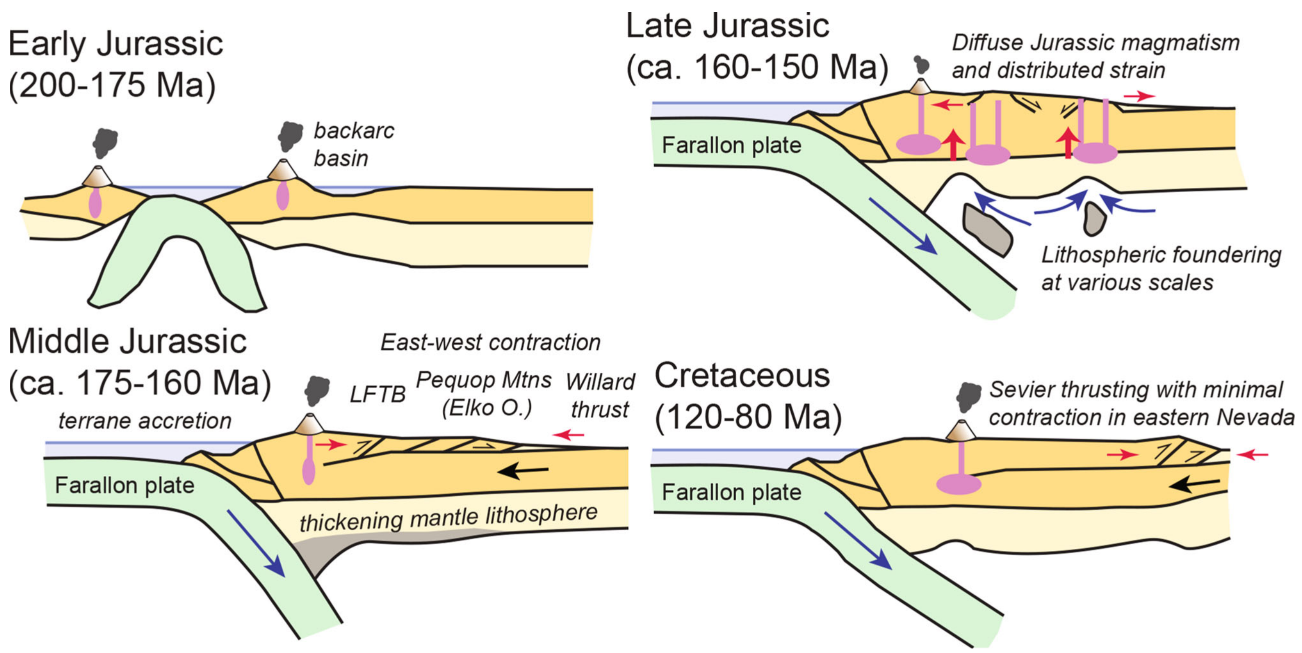

Figure 8: Schematic models of Mesozoic tectonics of the North American Cordillera, across the approximate latitude of 41°N. LFTB: Luning-Fencemaker thrust belt.

in western Nevada [133] and coeval strain to the south [134] and east [61, 135]. Middle-Late Jurassic deformation, distributed across the proto-Nevadaplano in the retroarc of the early Sierran magmatic arc (Figure 8), accommodated significant shortening, including ~50% strain in the Luning-Fencemaker thrust belt [133] and 20–30% strain in eastern NV-western Utah [61], and up to ~10 km shortening in Utah on the Willard thrust [135] (Figures 1 and 8). Together, this equates to ~100 km minimum shortening assuming a restored pre-Cenozoic width [43] (Figure 8).

The timing of much of this Jurassic deformation is not tightly constrained, except having occurred before ca. 155 Ma in most localities [32, 61]. Accordingly, Jurassic shortening may have been focused over a relatively narrow 170–155 Ma time range, which overlaps with contemporaneous terrane accretion in the Sierran forearc [136], increased North American-Farallon convergence rates (e.g., [56]), enhanced Jurassic arc magmatism, and a marked increase in crustal thickness in the Sierran arc [137–140] (Figures 1 and 7). This strong correlation is consistent with a broader Cordilleran cyclicity model [138, 141]. Alternatively, limited temporal-spatial constraints on Jurassic deformation permit relatively continuous, or semicontinuous, pulses of Middle-Late Jurassic to Late Cretaceous Cordilleran shortening [44]. Although this study has focused on Jurassic deformation in the Pequop Mountains and northeast Nevada-Utah, demonstrable Late Cretaceous strain is recorded in the Ruby Mountains-East Humboldt Range and across Nevada-Utah as documented by many workers (e.g., [16, 56]) (Figure 1(b)). In the Ruby Mountains-East Humboldt Range, this includes thrust faults that have been folded and intruded by Late Cretaceous peraluminous melts (e.g., [25, 45]). Across central Utah and Nevada, upper crustal shortening was pervasive (e.g., [52, 56, 124, 126, 142]) (Figure 1(b)). Taken together, this suggests that shortening strain at REWP latitudes occurred either (1) progressively from the Middle Jurassic to Late Cretaceous or (2) as two punctuated pulses of Jurassic and Cretaceous deformation (Figure 1(b)).

Middle-Late Jurassic upper crustal shortening of ~30% strain in eastern Nevada should have resulted in crustal thickening either via *in situ* pure-shear thickening [83, 130] or by feeding slip eastward to allow westward underthrusting of thick North American basement [44]. Therefore, based on the two strain-evolution scenarios stated above (i.e., progressive or punctuated pulses), we posit that growth of the Nevadaplano involved either protracted Jurassic-Cretaceous thickening or a dynamic pulsed evolution with growth phases separated by relative quiescence (dashed curves 2 or 3 in Figure 1(a)). The tight correlation of ca. 170–155 Ma punctuated events (Figure 1) may better support the pulsed-growth model. Either model differs from traditional models of restricted Late Cretaceous plateau growth ([28, 56]; curve 1 in Figure 1(a)) and highlights that crustal thickening in the Sierran retroarc was protracted and complex.

Crustal thickening probably varied spatially and temporally across present-day eastern California-Nevada-Utah, and based on this study and other published observations, it is clear that both Middle-Late Jurassic and Late Cretaceous deformation contributed to crustal thickening. Furthermore, this thickening spanned the width of the (proto) Nevadaplano early in its history—that is, deformation occurred 100's of km inboard of the western plate boundary in the Late Jurassic and Late Cretaceous—which suggests that the deformation front did not progressively migrate eastward through time. Such an observation is counter to thin-viscous sheet models for continental deformation and crustal thickening [143], highlights the significance of the out-of-sequence development of orogenic plateaus [52, 83, 144], and supports the idea that plate-boundary stresses can transfer rapidly across contractional settings to generate wide zones of intracontinental deformation [13]. Notably, this ca. 100 Myr long plateau evolution provides perspectives for modern orogenic plateaus that are in their infancy, such as the Andes or Tibet (Figure 1).

4.4. Implications for Refuting Postulated Deep Burial. Our observations also allow us to make interpretations regarding the more complexly deformed REWP geology. The Neoproterozoic-Cambrian rocks exposed along the western flank of the Pequop Mountains are the same rock types as those in the Wood Hills, and the garnet-/tremolite-in metamorphic isograds in the westernmost Pequop Mountains are thought to correspond to those identified in the Wood Hills [30, 54]. There is no major structure between the Wood Hills and Pequop Mountains, beside the west-dipping high-angle normal faults located along the western flank of the Pequop Mountains. Therefore, the Wood Hills and western Pequop Mountains represent similar structural levels (Figure 2). The Wood Hills rocks may have been slightly hotter, based on thermometry results of ~600°C ([23, 54]; cf. Figure 6(a) of this study), due to the proximity to the pervasively intruded Ruby Mountains-East Humboldt Range. Accordingly, ~6+ kbar pressure estimates from Neoproterozoic and Cambrian strata [23, 30] should approximately reflect pressures experienced by rocks in both the Wood Hills and Pequop Mountains. If lithostatic, these pressures imply burial to >22 km depths (ρ: 2.7 g/cm^3). Several observations presented here dispute such deep burial:

(1) Regionally, prograde *P-T-t* paths suggest that peak pressures were attained in the Late Cretaceous [25, 48], but our field observations only identify a significant phase of Jurassic contraction in the Pequop Mountains, with negligible Cretaceous deformation

(2) Depth-T_p relationships preclude deep burial of the strata in the Pequop Mountains, beyond the ~2 km burial recorded by the Jurassic Independence thrust and coeval structures (Figure 6). Pervasive Cretaceous intrusions in the Ruby Mountains-East Humboldt Range [25, 36] may have locally thickened the crust by several kilometers, but it is difficult to envision how this could bury rocks > 20 km deep

(3) Stratigraphy in the Pequop Mountains is continuous from the lower ZЄ Prospect Mountain Quartzite, with estimated ~6+ kbar peak pressures, upsection to undeformed Triassic rocks across an ~8 km thick section (Figure 2), which is at odds with deep burial. Also problematic are the lack of any surface exposures of the hypothesized Windermere thrust and inconsistency of its purported geometry with regional field relationships (Figure 2)

In the greater REWP region, peak *P-T* conditions for the lower ZЄ stratigraphy fall into two categories. Higher pressure estimates suggest 6–8+ kbar and 500–700°C [23, 25, 48, 50], whereas moderate pressure estimates suggest 3–4 kbar and 500–600°C [57, 58, 145]. Notably, the higher pressure estimates require geothermal gradients of 20–25°C/km, whereas the moderate pressure estimates suggest gradients of 30–50°C/km. Based on our observed temperature versus stratigraphic depth compilation that suggests relatively high geothermal gradients of ~40-50°C/km in the Pequop Mountains, we argue that the colder geothermal gradients implied by the higher pressure estimates are improbable, especially given the volume of intrusions in the Ruby Mountains-East Humboldt Range.

The Snake Range core complex to the south in eastern Nevada has a similar debate (Figure 2). Geobarometry suggests that the exposed ZЄ Prospect Mountain Quartzite and underlying Z McCoy Creek Group experienced pressures > 8 kbar and was apparently buried to depths three times stratigraphic depths [22, 24]. However, palinspastic reconstructions based on detailed field mapping are at odds with this deep burial [123, 146]. It remains unclear why field relationships prohibiting deep burial are so highly discrepant with high pressures recorded by geobarometers across NV core complexes, but the striking similarity between the REWP and Snake Range core complexes suggests that similar processes are operating in both localities.

Importantly, burial depth impacts the required magnitudes of Cenozoic extension necessary to exhume rocks to the surface. Models of 30+ km of vertical exhumation suggest that a substantial part of this had to have occurred since the early Eocene (e.g., [25]), which left a negligible record of Eocene basin deposits [49, 147]. Conversely, Miocene to present extension resulted in thick basins that are distributed across eastern Nevada (Figure 2) (e.g., [17, 49, 148]). Accordingly, negligible tectonic burial of the upper crust, as argued for in this study, is consistent with predominantly late Oligocene-Miocene, extension initiation across the Basin and Range [44, 149]. The main mylonitic detachment in the REWP was primarily active from 29 to 23 Ma based on crosscutting relationships involving U-Pb zircon-dated intrusive rocks [38, 150]. Zircon and apatite (U-Th)/He dating from the Ruby Mountains demonstrates exhumation initiated in the late Oligocene-early Miocene [151], and low-temperature thermochronology across the southern Ruby Mountains suggests rapid cooling-related to extension 17–15 Ma [51]. The high thermal gradients documented in this study (>40°C/km) complicate interpretations of lower temperature thermochronometers given that conductive cooling of the crust could affect measured ages, and we emphasize that thermochronology studies must be careful to differentiate and interpret exhumation versus crustal cooling.

Late Oligocene-Miocene extension initiation of moderate magnitudes (<15 km vertical exhumation) bears on the debate regarding driving mechanisms for Basin and Range extension (e.g., [17]). Moderate magnitude extension starting in the late Oligocene-Miocene is incompatible with models based solely on gravitational collapse of thickened crust driving extension (e.g., [18, 152]), which predict that extension should have initiated shortly after peak thickening in the Late Cretaceous-early Cenozoic (Figure 1). Instead, initiation of widespread extension in the Miocene supports models relating extension to changes in relative plate motion (e.g., [17, 153, 154]), although gravitational potential energy may have been an important driving force. In summary, most available data suggest that the basal ZЄ stratigraphy was exhumed from depth starting in the late Oligocene-Miocene time, significantly after Mesozoic crustal thickening, during a reorganization of plate-boundary conditions [153]. Existing exhumation models are more compatible with the lower stratigraphy rocks being exhumed from depths of <15 km (e.g., [145, 155]), which further supports the assertion that the basal ZЄ stratigraphy was not buried to great depths.

Lastly, we propose that the disconnect between high pressures recorded by multiple geobarometers and field relationships prohibiting deep burial across NV core complexes supports models of tectonic overpressure (e.g., [33, 34, 156, 157]). That is, the rocks recorded dynamic pressures rather than lithostatic overburden. Scenarios that may favor overpressure include regions adjacent to thickened plateaus [158], local melt generation and associated volume increase [159], or shear zones consisting of rocks with heterogeneous strengths [35, 157]. Yamato and Brun [160] argued that switching tectonic regimes from contraction to extension can lead to dynamic apparent pressure values that are higher than lithostatic pressures, and the magnitude of this effect is ultimately controlled by the strength, or differential stress, of the rock. These conditions directly apply to the geology of Nevadan core complexes. Specifically, the metamorphic rocks in Nevadan core complexes formed in regions adjacent to, or within, thickened crust of the Nevadaplano plateau (Figure 1) were associated with contractional-mode deformation during plateau construction and extension-mode strain during extension and are associated with voluminous intrusions including Cretaceous leucogranites that comprise significant volumes of the REWP crust [25]. The stratigraphy of northeast Nevada has highly variable strength, possibly enhancing overpressure (e.g., [35, 157, 161]), with weaker carbonates commonly flowing around more competent dolomite and quartzite as observed in the Pequop Mountains. In the Pequop Mountains, the entire ~10 m+ cliffs of quartzite and dolomite are boudinaged and apparently disappear on the map scale, with carbonate layers flowing around the rigid boudins [68]. The gold deposits at Long Canyon are postulated to have concentrated in the necks of these large-scale boudins [71].

Although overpressure concepts are highly controversial [162–164], the long-standing differences between pressures and field relationships in eastern NV may be a critical field test of overpressure hypotheses. We suggest that tectonic overpressure reconciles disparate field and petrologic observations. Alternatives are that field geologists are missing major structures and key field relationships or that geobarometric estimates neglect important considerations, such as reaction overstepping [165]. Future research considering these concepts may shed light on these controversies.

5. Conclusions

The Pequop Mountains comprise the least-deformed eastern flank of the REWP core complex, NE Nevada. In this study, we demonstrate that the main phase of contractional deformation in the Pequop Mountains occurred in the Middle-Late Jurassic, as demonstrated by a ca. 160 Ma lamprophyre sill that intruded a major southeast-directed mappable thrust fault, the Independence thrust. Jurassic deformation in the Pequop Mountains correlates with coeval Jurassic structures spanning from western Nevada to central Utah, which cumulatively accommodated at least 100 km of crustal shortening. Jurassic deformation was clearly significant in the Cordilleran hinterland. Although we found no evidence of major Cretaceous deformation in the Pequop Mountains, observations of Cretaceous strain distributed elsewhere across Nevada and localized along Sevier structures in Utah demonstrate a major pulse of Late Cretaceous shortening that affected the Cordilleran hinterland. We argue that pulsed Middle-Late Jurassic and Late Cretaceous deformation affected the Sierra Nevada retroarc, and models for the growth of the Nevadaplano orogenic plateau should consider this longer history.

We also present three primary lines of evidence from the Pequop Mountains that suggest that the Neoproterozoic-Triassic passive margin sequence of the REWP core complex was not buried significantly deeper than its original stratigraphic thickness. First, we cannot find direct field evidence for the proposed Windermere thrust, which would have doubled or tripled the stratigraphy. Stratigraphy is continuous over an ~8 km thick section from the metamorphosed and sheared Neoproterozoic-Cambrian Prospect Mountain Quartzite exposed on the western flank of the Pequop Mountains to internally undeformed Permian-Triassic strata in the central-southern and eastern parts of the range. Second, peak temperature data spanning the Cambrian-Permian section define a warm geothermal gradient (>40-50°C/km), consistent with the numerous intrusions and significant mineralization in the area, that is incompatible with burial by >15 km of duplicated stratigraphy. Lastly, crustal thickening and major shortening in the Pequop Mountains appear to have occurred in the Middle-Late Jurassic, not the Late Cretaceous as originally proposed, and thus, the inferred depth-time paths of these rocks must be reconsidered.

Limited burial of the passive margin sequence implies lower magnitudes of extension across the REWP that may have initiated in the Oligocene-Miocene, consistent with the history of deposition in regional extensional basins. These extensional characteristics support that extension was primarily controlled by changes in plate-boundary conditions, possibly facilitating gravitational collapse, rather than being solely driven by gravitational collapse. In both the REWP and Snake Range core complexes, palinspastic reconstructions of tectonic burial based on geologic mapping and field relationships are significantly discrepant from burial depths inferred from peak pressure estimates recorded by various barometers. We suggest that these disparities may reflect tectonic overpressure, where the rocks record dynamic pressures that exceed lithostatic pressures. Future research that incorporates overpressure models may shed light on this issue.

Data Availability

Data supporting the results of this study can be found in this manuscript text, the supplemental material file, previous publications discussed in the text, and published geologic maps accessed at http://www.nbmg.unr.edu/Maps&Data/.

Disclosure

The views and conclusions contained in this document are those of the authors and should not be interpreted as necessarily representing the official policies, either expressed or implied, of the U.S. Government.

Conflicts of Interest

The authors declare that they have no conflicts of interest.

Acknowledgments

We thank Art Snoke and all of his past students for illuminating the complex geology of the Ruby Mountains-East Humboldt Range, for him taking the time to show us some of the wonderful geology of the area, and for his detailed formal review of this manuscript. Tom Anderson, Fred Zoerner, and Steve Ruppel are also thanked for great discussions in the field, and Jeff Blackmon helped us with geologic discussions and access for the geology in the Long Canyon mine. Matt Heizler and Bill McIntosh are thanked for their guidance with argon analyses at New Mexico Tech. This research was partially supported by the USGS National Cooperative Geologic Mapping Program via StateMap awards (G14AC00237, G16AC00186, G17AC00212, G18AC00198, and G19AC00383) and by the National Science Foundation's Tectonics (EAR 1830139) and AGeS2 (EAR 1759200, 1759353, and 1759201) programs.

Supplementary Materials

Complete stratigraphic column, data tables for $^{40}Ar/^{39}Ar$, Raman spectroscopy on carbonaceous material, conodont color alteration index analyses, and peak-temperature synthesis. *(Supplementary Materials)*

References

[1] R. Bilham, V. K. Gaur, and P. Molnar, "Earthquakes: Himalayan seismic hazard," *Science*, vol. 293, no. 5534, pp. 1442–1444, 2001.

[2] B. A. Brooks, M. Bevis, K. Whipple et al., "Orogenic-wedge deformation and potential for great earthquakes in the central Andean backarc," *Nature Geoscience*, vol. 4, no. 6, pp. 380–383, 2011.

[3] K. A. Howard, "Crustal structure in the Elko-Carlin region, Nevada, during Eocene gold mineralization: Ruby-East Humboldt metamorphic core complex as a guide to the deep crust," *Economic Geology*, vol. 98, no. 2, pp. 249–268, 2003.

[4] X. Qu, Z. Hou, and Y. Li, "Melt components derived from a subducted slab in late orogenic ore-bearing porphyries in the Gangdese copper belt, southern Tibetan plateau," *Lithos*, vol. 74, no. 3-4, pp. 131–148, 2004.

[5] J. P. Richards, "Magmatic to hydrothermal metal fluxes in convergent and collided margins," *Ore Geology Reviews*, vol. 40, no. 1, pp. 1–26, 2011.

[6] P. Molnar, W. R. Boos, and D. S. Battisti, "Orographic controls on climate and paleoclimate of Asia: thermal and mechanical roles for the Tibetan Plateau," *Annual Review of Earth and Planetary Sciences*, vol. 38, no. 1, pp. 77–102, 2010.

[7] W. F. Ruddiman, *Tectonic Uplift and Climate Change*, Plenum Press, New York, 1997.

[8] K. C. Condie, *Plate Tectonics and Crustal Evo-lution*, Butterworth-Heinemann, Oxford, UK, 4th edition, 2003.

[9] S. R. Taylor and S. M. McLennan, "The geochemical evolution of the continental crust," *Reviews of Geophysics*, vol. 33, no. 2, pp. 241–265, 1995.

[10] G. A. Davis and G. S. Lister, "Detachment faulting in continental extension; perspectives from the southwestern U.S. Cordillera," *Processes in Continental Lithospheric Deformation*, vol. 218, pp. 133–160, 1988.

[11] P. Molnar, "Continental tectonics in the aftermath of plate tectonics," *Nature*, vol. 335, no. 6186, pp. 131–137, 1988.

[12] L. Royden, "Coupling and decoupling of crust and mantle in convergent orogens: implications for strain partitioning in the crust," *Journal of Geophysical Research: Solid Earth*, vol. 101, no. B8, pp. 17679–17705, 1996.

[13] M. K. Clark, "Continental collision slowing due to viscous mantle lithosphere rather than topography," *Nature*, vol. 483, no. 7387, pp. 74–77, 2012.

[14] C. N. Garzione, N. McQuarrie, N. D. Perez et al., "Tectonic evolution of the Central Andean plateau and implications for the growth of plateaus," *Annual Review of Earth and Planetary Sciences*, vol. 45, no. 1, pp. 529–559, 2017.

[15] P. Tapponnier, X. Zhiqin, F. Roger et al., "Oblique stepwise rise and growth of the Tibet plateau," *Science*, vol. 294, no. 5547, pp. 1671–1677, 2001.

[16] P. G. DeCelles, "Late Jurassic to Eocene evolution of the Cordilleran thrust belt and foreland basin system, western U.S.A," *American Journal of Science*, vol. 304, no. 2, pp. 105–168, 2004.

[17] J. P. Colgan and C. D. Henry, "Rapid middle Miocene collapse of the Mesozoic orogenic plateau in north-central Nevada," *International Geology Review*, vol. 51, no. 9-11, pp. 920–961, 2009.

[18] C. H. Jones, L. J. Sonder, and J. R. Unruh, "Lithospheric gravitational potential energy and past orogenesis: implications for conditions of initial Basin and Range and Laramide deformation," *Geology*, vol. 26, no. 7, pp. 639–642, 1998.

[19] R. L. Armstrong and E. Hansen, "Cordilleran infrastructure in the eastern Great Basin," *American Journal of Science*, vol. 264, no. 2, pp. 112–127, 1966.

[20] P. J. Coney and T. A. Harms, "Cordilleran metamorphic core complexes: Cenozoic extensional relics of Mesozoic compression," *Geology*, vol. 12, no. 9, pp. 550–554, 1984.

[21] E. L. Miller and P. B. Gans, "Cretaceous crustal structure and metamorphism in the hinterland of the Sevier thrust belt,

western U.S. Cordillera," *Geology*, vol. 17, no. 1, pp. 59–62, 1989.

[22] F. J. Cooper, J. P. Platt, R. Anczkiewicz, and M. J. Whitehouse, "Footwall dip of a core complex detachment fault: thermobarometric constraints from the northern Snake Range (Basin and Range, USA)," *Journal of Metamorphic Geology*, vol. 28, no. 9, pp. 997–1020, 2010.

[23] K. V. Hodges, A. W. Snoke, and H. A. Hurlow, "Thermal evolution of a portion of the Sevier hinterland: the northern Ruby Mountains-East Humboldt Range and Wood Hills, northeastern Nevada," *Tectonics*, vol. 11, no. 1, pp. 154–164, 1992.

[24] C. J. Lewis, B. P. Wernicke, J. Selverstone, and J. M. Bartley, "Deep burial of the footwall of the northern Snake Range decollement, Nevada," *Geological Society of America Bulletin*, vol. 111, no. 1, pp. 39–51, 1999.

[25] A. J. McGrew, M. T. Peters, and J. E. Wright, "Thermobarometric constraints on the tectonothermal evolution of the East Humboldt Range metamorphic core complex, Nevada," *Geological Society of America Bulletin*, vol. 112, no. 1, pp. 45–60, 2000.

[26] M. G. Best, D. L. Barr, E. H. Christiansen, S. Gromme, A. L. Deino, and D. G. Tingey, "The Great Basin Altiplano during the middle Cenozoic ignimbrite flareup: insights from volcanic rocks," *International Geology Review*, vol. 51, no. 7-8, pp. 589–633, 2009.

[27] C. P. Chamberlain, H. T. Mix, A. Mulch et al., "The Cenozoic climatic and topo-graphic evolution of the western North American Cordillera," *American Journal of Science*, vol. 312, no. 2, pp. 213–262, 2012.

[28] J. B. Chapman, M. N. Ducea, P. G. DeCelles, and L. Profeta, "Tracking changes in crustal thickness during orogenic evolution with Sr/Y: an example from the North American Cordillera," *Geology*, vol. 43, no. 10, pp. 919–922, 2015.

[29] K. E. Snell, P. L. Koch, P. Druschke, B. Z. Foreman, and J. M. Eiler, "High elevation of the 'Nevadaplano' during the Late Cretaceous," *Earth and Planetary Science Letters*, vol. 386, pp. 52–63, 2014.

[30] P. A. Camilleri and K. R. Chamberlain, "Mesozoic tectonics and metamorphism in the Pequop Mountains and Wood Hills region, northeast Nevada: implications for the architecture and evolution of the Sevier orogen," *Geological Society of America Bulletin*, vol. 109, no. 1, pp. 74–94, 1997.

[31] C. H. Thorman, "Some musings regarding structural evolution of NE Nevada-NW Utah from Jurassic to Recent," *Geological Society of America, Rocky Mountain and Cordilleran Section Meeting*, vol. 43, no. 4, p. 3, 2011.

[32] C. H. Thorman, K. B. Ketner, W. E. Brooks, L. W. Snee, and R. A. Zimmerman, "Late Mesozoic-Cenozoic tectonics in northeastern Nevada," in *Geology and ore deposits of the Great Basin: Symposium Proceedings*, G. K. Raines, Ed., vol. 1, pp. 25–45, Geological Society of Nevada, Reno, NV, USA, 1991.

[33] T. Gerya, "Tectonic overpressure and underpressure in lithospheric tectonics and metamorphism," *Journal of Metamorphic Geology*, vol. 33, no. 8, pp. 785–800, 2015.

[34] K. Petrini and Y. Y. Podladchikov, "Lithospheric pressure-depth relationship in compressive regions of thickened crust," *Journal of Metamorphic Geology*, vol. 18, no. 1, pp. 67–77, 2000.

[35] S. M. Schmalholz and Y. Y. Podladchikov, "Tectonic overpressure in weak crustal-scale shear zones and implications for the exhumation of high-pressure rocks," *Geophysical Research Letters*, vol. 40, no. 10, pp. 1984–1988, 2013.

[36] K. A. Howard, J. L. Wooden, C. G. Barnes, W. R. Premo, A. W. Snoke, and S. Y. Lee, "Episodic growth of a Late Cretaceous and Paleogene intrusive complex of pegmatitic leucogranite, Ruby Mountains core complex, Nevada, USA," *Geosphere*, vol. 7, no. 5, pp. 1220–1248, 2011.

[37] S. Y. Lee, C. G. Barnes, A. W. Snoke, K. A. Howard, and C. D. Frost, "Petrogenesis of Mesozoic, peraluminous granites in the Lamoille Canyon area, Ruby Mountains, Nevada, USA," *Journal of Petrology*, vol. 44, no. 4, pp. 713–732, 2003.

[38] J. E. Wright and A. W. Snoke, "Tertiary magmatism and mylonitization in the Ruby-East Humboldt metamorphic core complex, northeastern Nevada: U-Pb geochronology and Sr, Nd, and Pb isotope geochemistry," *Geological Society of America Bulletin*, vol. 105, no. 7, pp. 935–952, 1993.

[39] G. H. Davis and P. J. Coney, "Geologic development of the Cordilleran metamorphic core complexes," *Geology*, vol. 7, no. 3, pp. 120–124, 1979.

[40] K. A. Howard, "Metamorphic infrastructure in the northern Ruby Mountains, Nevada," *Geological Society of America Memoir*, vol. 153, pp. 335–347, 1980.

[41] A. W. Snoke, A. J. McGrew, P. A. Valasek, and S. B. Smithson, "A crustal cross-section for a terrain of superimposed shortening and extension: Ruby Mountains-East Humboldt Range metamorphic core complex, Nevada," in *Exposed cross sections of the continental crust: NATO ASI Series (Series C: Mathematical and Physical Sciences)*, M. H. Salisbury and D. M. Fountain, Eds., pp. 103–135, Springer, Dordrecht, 1990.

[42] A. W. Snoke, K. A. Howard, A. J. McGrew et al., "The grand tour of the Ruby-East Humboldt metamorphic core complex, northeastern Nevada," in *Proterozoic to recent stratigraphy, tectonics, and volcanology, Utah, Nevada, southern Idaho, and central Mexico*, P. K. Link and B. J. Kowalis, Eds., vol. 42, pp. 225–269, Brigham Young University Geology Studies, 1997, Part I.

[43] N. McQuarrie and B. P. Wernicke, "An animated tectonic reconstruction of southwestern North America since 36 Ma," *Geosphere*, vol. 1, no. 3, pp. 147–172, 2005.

[44] S. P. Long, "Geometry and magnitude of extension in the Basin and Range Province (39°N), Utah, Nevada, and California, USA: constraints from a province-scale cross section," *Geological Society of America Bulletin*, vol. 131, no. 1-2, pp. 99–119, 2019.

[45] A. J. McGrew and A. W. Snoke, *Geologic map of the Welcome quadrangle and an adjacent part of the Wells quadrangle, Elko County, Nevada*, Nevada Bureau of Mines and Geology, 2015, Map 184, scale 1:24,000.

[46] J. H. Stewart and F. G. Poole, "Lower Paleozoic and uppermost Precambrian Cordilleran miogeocline, Great Basin, western United States," in *Tectonics and Sedimentation*, W. R. Dickinson, Ed., vol. 22, pp. 28–57, Society of Economic Paleontologists and Mineralogists (SEPM) Special Publication, 1974.

[47] P. Camilleri, *Geologic map of the northern Pequop Mountains, Elko County, Nevada*, Nevada Bureau of Mines and Geology Map 171, scale 1:48,000, 2010.

[48] B. W. Hallett and F. S. Spear, "The P–T history of anatectic pelites of the Northern East Humboldt Range, Nevada:

evidence for tectonic loading, decompression, and Anatexis," *Journal of Petrology*, vol. 55, no. 1, pp. 3–36, 2014.

[49] C. D. Henry, A. J. McGrew, J. P. Colgan, A. W. Snoke, and M. E. Brueseke, "Timing, distribution, amount, and style of Cenozoic extension in the northern Great Basin," in *Geologic Field Trips to the Basin and Range, Rocky Mountains, Snake River Plain, and Terranes of the U.S. Cordillera*, J. Lee and J. P. Evans, Eds., vol. 21, pp. 27–66, Geological Society of America Field Guide, 2011.

[50] B. W. Hallett and F. S. Spear, "Monazite, zircon, and garnet growth in migmatitic pelites as a record of metamorphism and partial melting in the East Humboldt Range, Nevada," *American Mineralogist*, vol. 100, no. 4, pp. 951–972, 2015.

[51] J. P. Colgan, K. A. Howard, R. J. Fleck, and J. L. Wooden, "Rapid middle Miocene extension and unroofing of the southern Ruby Mountains, Nevada," *Tectonics*, vol. 29, no. 6, 2010.

[52] S. P. Long, C. D. Henry, J. L. Muntean, G. P. Edmondo, and E. J. Cassel, "Early Cretaceous construction of a structural culmination, Eureka, Nevada, U.S.A.: implications for out-of-sequence deformation in the Sevier hinterland," *Geosphere*, vol. 10, no. 3, pp. 564–584, 2014.

[53] W. R. Premo, P. Castiñeiras, and J. L. Wooden, "SHRIMP-RG U-Pb isotopic systematics of zircon from the Angel Lake orthogneiss, East Humboldt Range, Nevada: is this really Archean crust?," *Geosphere*, vol. 4, no. 6, pp. 963–975, 2008.

[54] M. A. Wills, *A metamorphic pressure-temperature time path from the Wood Hills, Elko County, eastern Nevada, [M.S. thesis]*, Northern Arizona University, 2014.

[55] P. Camilleri, A. Yonkee, J. Coogan, P. DeCelles, A. McGrew, and M. Wells, "Hinterland to foreland transect through the Sevier Orogen, northeast Nevada to north central Utah: structural style, metamorphism, and kinematic history of a large contractional orogenic wedge," *Brigham Young University Geology Studies*, vol. 42, pp. 297–309, 1997.

[56] W. A. Yonkee and A. B. Weil, "Tectonic evolution of the Sevier and Laramide belts within the North American Cordillera orogenic system," *Earth-Science Reviews*, vol. 150, pp. 531–593, 2015.

[57] M. R. Hudec, "Mesozoic structural and metamorphic history of the central Ruby Mountains metamorphic core complex, Nevada," *Geological Society of America Bulletin*, vol. 104, no. 9, pp. 1086–1100, 1992.

[58] J. V. Jones III, *Deformational, magmatic, and metamorphic history of the central Ruby Mountains, Elko County, Nevada, [M.S. thesis]*, University of Wyoming, Laramie, 1999.

[59] R. W. Allmendinger and T. E. Jordan, "Mesozoic structure of the Newfoundland Mountains, Utah: horizontal shortening and subsequent extension in the hinterland of the Sevier belt," *Geological Society of America Bulletin*, vol. 95, no. 11, pp. 1280–1292, 1984.

[60] D. M. Miller and T. D. Hoisch, "Mesozoic structure, metamorphism, and magmatism in the Pilot and Toano Ranges. Field guide to geologic excursions in Utah and adjacent areas of Nevada, Idaho, and Wyoming," *Utah Geological Survey Miscellaneous Publication*, vol. 92, no. 3, pp. 79–92, 1992.

[61] D. M. Miller and T. D. Hoisch, "Jurassic tectonics of northeastern Nevada and northwestern Utah from the perspective of barometric studies," *Jurassic magmatism and tectonics of the North American Cordillera: Geological Society of America Special Paper*, vol. 299, pp. 267–294, 1995.

[62] C. H. Thorman and F. Peterson, "The Middle Jurassic Elko orogeny: a major tectonic event in Nevada-Utah," *AAPG Annual Meeting Expanded Abstracts*, vol. 12, pp. 169–174, 2003.

[63] C. H. Thorman, K. B. Ketner, and F. Peterson, "The Elko orogeny - Late Jurassic orogenesis in the Cordilleran miogeocline," vol. 22, Tech. Rep. 3, , Geological Society of America, Cordilleran Section Meeting, Tucson, Arizona, 1990.

[64] C. H. Thorman, *Structure and stratigraphy of the Wood Hills and a portion of the northern Pequop Mountains, Elko County, Nevada, [Ph.D. thesis]*, University of Washington, Seattle, 1962.

[65] C. H. Thorman, "Metamorphosed and nonmetamorphosed Paleozoic rocks in the Wood Hills and Pequop Mountains, northeast Nevada," *Geological Society of America Bulletin*, vol. 81, no. 8, pp. 2417–2448, 1970.

[66] P. A. Camilleri, *Mesozoic and Cenozoic tectonic and metamorphic evolution of the Wood Hills and Pequop Mountains. Elko County, Nevada, [PhD Dissertation]*, University of Wyoming, Laramie, 1994.

[67] J. Wise, "Mesozoic tectonics and metamorphism in the Pequop Mountains and Wood Hills region, northeast Nevada: implications for the architecture and evolution of the Sevier orogen: Discussion," *Geological Society of America Bulletin*, vol. 110, no. 5, pp. 679-680, 1998.

[68] A. V. Zuza, C. D. Henry, M. W. Ressel, C. H. Thorman, S. Dee, and J. E. Blackmon, *Preliminary geologic map of the Independence Valley NE quadrangle, Elko County, Nevada*, Nevada Bureau of Mines and Geology Open File Report 18-4, 2018, scale 1:24,000.

[69] R. Bedell, E. Struhsacker, L. Craig et al., "The Pequop mining district, Elko County, Nevada: an evolving new gold district," *Society of Economic Geologists Special Publication*, vol. 15, pp. 29–56, 2010.

[70] A. K. Milliard, M. W. Ressel, C. D. Henry, C. Ricks, and G. Loptien, "Age, distribution, and composition of igneous rocks of the Pequop Mountains, Northeast Nevada: association with Carlin-type gold deposits," in *Geological Society of Nevada, 2015 Symposium*, pp. 895–923, 2015.

[71] M. T. Smith, D. Rhys, K. Ross, C. Lee, and J. N. Gray, "The Long Canyon deposit: anatomy of a new off-trend sedimentary rock-hosted gold discovery in northeastern Nevada," *Economic Geology*, vol. 108, no. 5, pp. 1119–1145, 2013.

[72] W. E. Brooks, C. H. Thorman, and L. W. Snee, "The ^{40}Ar/^{39}Ar ages and tectonic setting of the middle Eocene northeast Nevada volcanic field," *Journal of Geophysical Research*, vol. 100, no. B6, pp. 10403–10416, 1995.

[73] W. E. Brooks, W. E. Thorman, L. W. Snee, C. W. Nutt, C. J. Potter, and R. F. Dubiel, "Summary of chemical analyses and 40Ar/39Ar-spectra data for Eocene volcanic rocks from the central part of the Northeast Nevada volcanic field," *U.S. Geological Survey Bulletin*, vol. 1988-K, pp. K1–K33, 1995.

[74] C. D. Henry and C. H. Thorman, *Preliminary geologic map of the Pequop Summit quadrangle, Elko County, Nevada*, Nevada Bureau of Mines and Geology Open File Report 15-8, scale 1:24,000, 2015.

[75] J. P. Colgan, C. D. Henry, and D. A. John, *Geologic map of the Caetano caldera, Lander and Eureka Counties, Nevada*, Nevada Bureau of Mines and Geology Map 174, 1:75,000, 2011.

[76] M. T. Fithian, E. A. Holley, and N. M. Kelly, "Geology of gold deposits at the Marigold mine, Battle Mountain district, Nevada," *Reviews in Economic Geology*, vol. 20, pp. 121–155, 2018.

[77] M. W. Ressel and C. D. Henry, "Igneous geology of the Carlin trend, Nevada: development of the Eocene plutonic complex and significance for Carlin-type gold deposits," *Economic Geology*, vol. 101, no. 2, pp. 347–383, 2006.

[78] K. A. Howard, *Structure of the Metamorphic Rocks of the Northern Ruby Mountains, Nevada [PhD Dissertation]*, Yale University, New Haven, Connecticut, 1966.

[79] K. R. Sicard, *The relationship between Cretaceous and Tertiary magmatism and structural development in the southeastern East Humboldt Range, part of the Ruby-East Humboldt core complex, Northeast Nevada, [M.S. thesis]*, University of Wyoming, Laramie, 2012.

[80] K. R. Sicard and A. Snoke, *Geology of the Gordon Creek Quadrangle*, Nevada Bureau of Mines and Geology Geologic, Elko County, Nevada, In press.

[81] H. A. Hurlow, *Structural geometry, fabric, and chronology of a Tertiary extensional shear zone-detachment system, southwestern East Humboldt Range, Elko County, Nevada, [M.S. thesis]*, University of Wyoming, 1987.

[82] A. J. McGrew, *Geologic map of the Humboldt Peak Quadrangle, Elko County, Nevada*, Nevada Bureau of Mines and Geology, 2018, Map 186, scale 1:24,000.

[83] A. V. Zuza, S. Dee, C. D. Henry, M. W. Ressel, and C. H. Thorman, *Geologic map of the Independence Valley NW quadrangle, Elko County, Nevada*, Nevada Bureau of Mines and Geology Open File Report 19-3, 2019, scale 1:24,000.

[84] C. D. Henry, "Ash-flow tuffs and paleovalleys in northeastern Nevada: implications for Eocene paleogeography and extension in the Sevier hinterland, northern Great Basin," *Geosphere*, vol. 4, no. 1, pp. 1–35, 2008.

[85] C. D. Henry, N. H. Hinz, J. E. Faulds et al., "Eocene–early Miocene paleotopography of the Sierra Nevada–Great Basin–Nevadaplano based on widespread ash-flow tuffs and paleovalleys," *Geosphere*, vol. 8, no. 1, pp. 1–27, 2012.

[86] W. C. McIntosh, M. Heizler, L. Peters, and R. Esser, *$^{40}Ar/^{39}Ar$ geochronology at the New Mexico Bureau of Geology and Mineral Resources*, New Mexico Bureau of Geology and Mineral Resources: Open File Report OF-AR-1, Socorro, 2003.

[87] C. D. Henry, S. B. Castor, W. A. Starkel et al., "Geology and evolution of the McDermitt caldera, northern Nevada and southeastern Oregon, western USA," *Geosphere*, vol. 13, no. 4, pp. 1066–1112, 2017.

[88] K. F. Kuiper, A. Deino, F. J. Hilgen, W. Krijgsman, P. R. Renne, and J. R. Wijbrans, "Synchronizing rock clocks of Earth history," *Science*, vol. 320, no. 5875, pp. 500–504, 2008.

[89] T. M. Harrison, "Diffusion of ^{40}Ar in hornblende," *Contributions to Mineralogy and Petrology*, vol. 78, no. 3, pp. 324–331, 1982.

[90] I. McDougall and T. M. Harrison, *Geochronology and Thermochronology by the $^{40}Ar/^{39}Ar$ Method*, Oxford University Press on Demand, 1999.

[91] T. M. Harrison, I. Duncan, and I. Mcdougall, "Diffusion of 40Ar in biotite: temperature, pressure and compositional effects," *Geochimica et Cosmochimica Acta*, vol. 49, no. 11, pp. 2461–2468, 1985.

[92] C. Howland, *High Thermal Gradient in the Upper Plate of a Core Complex, Determined by Calcite-Dolomite and RSCM Thermometry, Pequop Mountains, NV [BS Honors thesis]*, Union College, Schenectady, NY, USA, 2016.

[93] J. R. Latham, *Mechanisms and patterns of strain related to late Mesozoic tectonic shortening on the Independence Thrust, Pequop Mountains, Elko County Nevada*, vol. 29, Keck Geology Consortium Short Contributions, 2016.

[94] F. J. Cooper, K. V. Hodges, and B. A. Adams, "Metamorphic constraints on the character and displacement of the South Tibetan fault system, central Bhutanese Himalaya," *Lithosphere*, vol. 5, no. 1, pp. 67–81, 2013.

[95] S. P. Long, S. M. Gordon, J. P. Young, and E. Soignard, "Temperature and strain gradients through Lesser Himalayan rocks and across the Main Central thrust, south central Bhutan: implications for transport-parallel stretching and inverted metamorphism," *Tectonics*, vol. 35, no. 8, pp. 1863–1891, 2016.

[96] M. Aoya, Y. Kouketsu, S. Endo et al., "Extending the applicability of the Raman carbonaceous-material geothermometer using data from contact metamorphic rocks," *Journal of Metamorphic Geology*, vol. 28, no. 9, pp. 895–914, 2010.

[97] O. Beyssac, B. Goffé, C. Chopin, and J. N. Rouzaud, "Raman spectra of carbonaceous material in metasediments: a new geothermometer," *Journal of Metamorphic Geology*, vol. 20, no. 9, pp. 859–871, 2002.

[98] J. M. Rahl, K. M. Anderson, M. T. Brandon, and C. Fassoulas, "Raman spectroscopic carbonaceous material thermometry of low-grade metamorphic rocks: calibration and application to tectonic exhumation in Crete, Greece," *Earth and Planetary Science Letters*, vol. 240, no. 2, pp. 339–354, 2005.

[99] A. G. Epstein, J. B. Epstein, and L. D. Harris, *Conodont color alteration: an index to organic metamorphism*, Geological Survey Professional Paper 995, 1977.

[100] L. M. Anovitz and E. J. Essene, "Phase equilibria in the system CaCO3-MgCO3-FeCO3," *Journal of Petrology*, vol. 28, no. 2, pp. 389–415, 1987.

[101] K. B. Ketner, W. C. Day, M. Elrick et al., *An outline of tectonic, igneous, and metamorphic events in the Goshute-Toano range between Silver Zone pass and White Horse pass, Elko county, Nevada: a history of superposed contractional and extensional deformation*, US Geological Survey, 1998, no. 1593.

[102] M. Herwegh and O. A. Pfiffner, "Tectono-metamorphic evolution of a nappe stack: a case study of the Swiss Alps," *Tectonophysics*, vol. 404, no. 1-2, pp. 55–76, 2005.

[103] M. J. Bickle and R. Powell, "Calcite-dolomite geothermometry for iron-bearing carbonates," *Contributions to Mineralogy and Petrology*, vol. 59, no. 3, pp. 281–292, 1977.

[104] S. J. Covey-Crump and E. H. Rutter, "Thermally-induced grain growth of calcite marbles on Naxos Island, Greece," *Contributions to Mineralogy and Petrology*, vol. 101, no. 1, pp. 69–86, 1989.

[105] J. R. Goldsmith and R. C. Newton, "P–T–X relations in the system CaCO,-MgCO, at high temperatures and pressures," *American Journal of Science*, vol. 267-A, pp. 160–190, 1969.

[106] J. E. Lieberman and J. M. Rice, "Petrology of marble and peridotite in the Seiad ultramafic complex, northern California, USA," *Journal of Metamorphic Geology*, vol. 4, no. 2, pp. 179–199, 1986.

[107] H. Mori, N. Mori, S. Wallis, R. Westaway, and C. Annen, "The importance of heating duration for Raman CM

thermometry: evidence from contact metamorphism around the Great Whin Sill intrusion, UK," *Journal of Metamorphic Geology*, vol. 35, no. 2, pp. 165–180, 2017.

[108] D. K. Fisler and R. T. Cygan, "Diffusion of Ca and Mg in calcite," *American Mineralogist*, vol. 84, no. 9, pp. 1392–1399, 1999.

[109] T. Müller, D. Cherniak, and E. B. Watson, "Interdiffusion of divalent cations in carbonates: experimental measurements and implications for timescales of equilibration and retention of compositional signatures," *Geochimica et Cosmochimica Acta*, vol. 84, pp. 90–103, 2012.

[110] R. D. Hyndman, "Lower-crustal flow and detachment in the North American Cordillera: a consequence of Cordillera-wide high temperatures," *Geophysical Journal International*, vol. 209, no. 3, pp. 1779–1799, 2017.

[111] S. P. Long and E. Soignard, "Shallow-crustal metamorphism during Late Cretaceous anatexis in the Sevier hinterland plateau: peak temperature conditions from the Grant Range, eastern Nevada, U.S.A," *Lithosphere*, vol. 8, no. 2, pp. 150–164, 2016.

[112] W. D. Means, "Stretching faults," *Geology*, vol. 17, no. 10, pp. 893–896, 1989.

[113] A. A. G. Webb, A. Yin, T. M. Harrison et al., "Cenozoic tectonic history of the Himachal Himalaya (northwestern India) and its constraints on the formation mechanism of the Himalayan orogen," *Geosphere*, vol. 7, no. 4, pp. 1013–1061, 2011.

[114] E. A. du Bray, M. W. Ressel, and C. G. Barnes, "Geochemical database for intrusive rocks of north-central and northeast Nevada," USGS Data Series 244, 2007.

[115] D. M. Miller, J. K. Nakata, and L. L. Glick, "K-Ar ages of Jurassic to Tertiary plutonic and metamorphic rocks, northwestern Utah and northeastern Nevada," *U.S. Geological Survey Bulletin*, vol. 1906, p. 18, 1990.

[116] J. K. Mortensen, J. F. H. Thompson, and R. M. Tosdal, "U-Pb age constraints on magmatism and mineralization in the northern Great Basin, Nevada," *Geology and ore deposits 2000: The Great Basin and beyond: Geological Society of Nevada Symposium Proceedings*, J. K. Cluer, J. G. Price, E. M. Struhsacker, R. F. Hardyman, and C. L. Morris, Eds., pp. 419–438, 2000.

[117] C. H. Thorman, C. A. Sandberg, C. D. Henry, A. V. Zuza, and M. W. Ressel, "Regional tectonics and conodont CAIs indicate normal burial depths, not Mesozoic thickening, in the Pequop Mountains, NE Nevada," in *Cordilleran Section - 115th Annual Meeting - 2019*, vol. 51, Portland, OR, USA, 2019.

[118] S. P. Long, M. T. Heizler, S. N. Thomson, P. W. Reiners, and J. E. Fryxell, "Rapid Oligocene to early Miocene extension along the Grant Range detachment system, Nevada, USA: insights from multipart cooling histories of footwall rocks," *Tectonics*, vol. 37, no. 12, pp. 4752–4779, 2018.

[119] D. Blackwell, M. Richards, Z. Frone et al., "Temperature at depth maps for the conterminous US and geothermal resource estimates," *Geolthermal Resource Council Transactions*, vol. 35, 2011.

[120] A. H. Lachenbruch, "Heat flow in the Basin and Range province and thermal effects of tectonic extension," in *Geothermics and Geothermal Energy. Contributions to Current Research in Geophysics (CCRG)*, L. Rybach and L. Stegena, Eds., pp. 34–50, Birkhäuser, Basel, 1979.

[121] R. F. Swenson, *Analysis of a fault-fold system in the southern Pequop Mountains, Elko County, Nevada, [M.S. thesis]*, University of Wyoming, Laramie, 1991.

[122] R. L. Armstrong, "Sevier orogenic belt in Nevada and Utah," *Geological Society of America Bulletin*, vol. 79, no. 4, pp. 429–458, 1968.

[123] P. B. Gans and E. L. Miller, *Style of mid-Tertiary extension in east-central Nevada: Utah Geological and Mineral Survey Special Studies Guidebook, Part 1*, vol. 59, pp. 107–160, 1983.

[124] S. P. Long, "Magnitudes and spatial patterns of erosional exhumation in the Sevier hinterland, eastern Nevada and western Utah, USA: insights from a Paleogene paleogeologic map," *Geosphere*, vol. 8, no. 4, pp. 881–901, 2012.

[125] N. J. Van Buer, E. L. Miller, and T. A. Dumitru, "Early Tertiary paleogeologic map of the northern Sierra Nevada batholith and the northwestern Basin and Range," *Geology*, vol. 37, no. 4, pp. 371–374, 2009.

[126] S. P. Long, "An upper-crustal fold province in the hinterland of the Sevier orogenic belt, eastern Nevada, U.S.A.: a Cordilleran Valley and Ridge in the Basin and Range," *Geosphere*, vol. 11, no. 2, pp. 404–424, 2015.

[127] R. B. Anderson, S. P. Long, B. K. Horton, A. Z. Calle, and V. Ramirez, "Shortening and structural architecture of the Andean fold-thrust belt of southern Bolivia (21 S): implications for kinematic development and crustal thickening of the central Andes," *Geosphere*, vol. 13, no. 2, pp. 538–558, 2017.

[128] R. Gao, H. Wang, A. Yin et al., "Tectonic development of the northeastern Tibetan Plateau as constrained by high-resolution deep seismic-reflection data," *Lithosphere*, vol. 5, no. 6, pp. 555–574, 2013.

[129] C. Wang, R. Gao, A. Yin et al., "A mid-crustal strain-transfer model for continental deformation: a new perspective from high-resolution deep seismic-reflection profiling across NE Tibet," *Earth and Planetary Science Letters*, vol. 306, no. 3-4, pp. 279–288, 2011.

[130] A. V. Zuza, X. Cheng, and A. Yin, "Testing models of Tibetan Plateau formation with Cenozoic shortening estimates across the Qilian Shan–Nan Shan thrust belt," *Geosphere*, vol. 12, no. 2, pp. 501–532, 2016.

[131] A. V. Zuza, C. Wu, Z. Wang et al., "Underthrusting and duplexing beneath the northern Tibetan Plateau and the evolution of the Himalayan-Tibetan orogen," *Lithosphere*, vol. 11, no. 2, pp. 209–231, 2018.

[132] A. V. Zuza, C. Wu, R. C. Reith et al., "Tectonic evolution of the Qilian Shan: an early Paleozoic orogen reactivated in the Cenozoic," *Geological Society of America Bulletin*, vol. 130, no. 5-6, pp. 881–925, 2017.

[133] S. J. Wyld, "Structural evolution of a Mesozoic backarc fold-and-thrust belt in the US Cordillera: new evidence from northern Nevada," *Geological Society of America Bulletin*, vol. 114, no. 11, pp. 1452–1468, 2002.

[134] M. A. Giallorenzo, M. L. Wells, W. A. Yonkee, D. F. Stockli, and B. P. Wernicke, "Timing of exhumation, Wheeler Pass thrust sheet, southern Nevada and California: late Jurassic to middle Cretaceous evolution of the southern Sevier fold-and-thrust belt," *Geological Society of America Bulletin*, vol. 130, no. 3-4, pp. 558–579, 2017.

[135] W. A. Yonkee, B. Eleogram, M. L. Wells, D. F. Stockli, S. Kelley, and D. E. Barber, "Fault slip and exhumation history of the Willard Thrust sheet, Sevier fold-thrust belt, Utah:

relations to wedge propagation, hinterland uplift, and foreland basin sedimentation," *Tectonics*, vol. 38, no. 8, pp. 2850–2893, 2019.

[136] R. A. Schweickert, C. Merguerian, and N. L. Bogen, "Deformational and metamorphic history of Paleozoic and Mesozoic basement terranes in the western Sierra Nevada metamorphic belt," in *Metamorphism and Crustal Evolution of the Western United States: Englewood Cliffs*, W. G. Ernst, Ed., pp. 789–820, Prentice-Hall, New Jersey, 1988.

[137] W. Cao and S. Paterson, "A mass balance and isostasy model: exploring the interplay between magmatism, deformation and surface erosion in continental arcs using Central Sierra Nevada as a case study," *Geochemistry, Geophysics, Geosystems*, vol. 17, no. 6, pp. 2194–2212, 2016.

[138] P. G. DeCelles, M. N. Ducea, P. Kapp, and G. Zandt, "Cyclicity in Cordilleran orogenic systems," *Nature Geoscience*, vol. 2, no. 4, pp. 251–257, 2009.

[139] M. Kirsch, S. R. Paterson, F. Wobbe, A. M. M. Ardila, B. L. Clausen, and P. H. Alasino, "Temporal histories of Cordilleran continental arcs: testing models for magmatic episodicity," *American Mineralogist*, vol. 101, no. 10, pp. 2133–2154, 2016.

[140] L. Profeta, M. N. Ducea, J. B. Chapman et al., "Quantifying crustal thickness over time in magmatic arcs," *Scientific Reports*, vol. 5, article 17786, 2015.

[141] P. G. DeCelles and S. A. Graham, "Cyclical processes in the North American Cordilleran orogenic system," *Geology*, vol. 43, no. 6, pp. 499–502, 2015.

[142] D. C. Greene, "The Confusion Range, west-central Utah: fold-thrust deformation and a western Utah thrust belt in the Sevier hinterland," *Geosphere*, vol. 10, no. 1, pp. 148–169, 2014.

[143] P. England and G. Houseman, "Finite strain calculations of continental deformation: 2. Comparison with the India-Asia collision zone," *Journal of Geophysical Research*, vol. 91, no. B3, pp. 3664–3676, 1986.

[144] C. Wu, A. V. Zuza, Z. Zhou et al., "Mesozoic-Cenozoic evolution of the Eastern Kunlun Range, central Tibet, and implications for basin evolution during the Indo-Asian collision," *Lithosphere*, vol. 11, no. 4, pp. 524–550, 2019.

[145] H. A. Hurlow, A. W. Snoke, and K. V. Hodges, "Temperature and pressure of mylonitization in a Tertiary extensional shear zone, Ruby Mountains-East Humboldt Range, Nevada: tectonic implications," *Geology*, vol. 19, no. 1, pp. 82–86, 1991.

[146] E. L. Miller, P. B. Gans, and J. Garing, "The Snake Range décollement: an exhumed mid-Tertiary ductile-brittle transition," *Tectonics*, vol. 2, no. 3, pp. 239–263, 1983.

[147] J. E. Lund Snee, E. L. Miller, M. Grove, J. K. Hourigan, and A. Konstantinou, "Cenozoic paleogeographic evolution of the Elko Basin and surrounding region, northeast Nevada," *Geosphere*, vol. 12, no. 2, pp. 464–500, 2016.

[148] P. Camilleri, J. Deibert, and M. Perkins, "Middle Miocene to Holocene tectonics, basin evolution, and paleogeography along the southern margin of the Snake River Plain in the Knoll Mountain–Ruby–East Humboldt Range region, northeastern Nevada and south-central Idaho," *Geosphere*, vol. 13, no. 6, pp. 1901–1948, 2017.

[149] C. D. Henry and D. A. John, "Magmatism, ash-flow tuffs, and calderas of the ignimbrite flareup in the western Nevada volcanic field, Great Basin, USA," *Geosphere*, vol. 9, no. 4, pp. 951–1008, 2013.

[150] K. J. Mueller, P. K. Cerveny, L. W. Snee, and M. E. Perkins, "Chronology of polyphase extension in the Windermere Hills, northeast Nevada," *Geological Society of America Bulletin*, vol. 111, no. 1, pp. 11–27, 1999.

[151] C. Mueller, *Thermochronology of the deep crust in the northern Ruby Mountains, NV, [B.S. thesis]*, University of Colorado, Boulder, 2019.

[152] L. J. Sonder and C. H. Jones, "Western United States extension: how the west was widened," *Annual Review of Earth and Planetary Sciences*, vol. 27, no. 1, pp. 417–462, 1999.

[153] T. Atwater, "Implications of plate tectonics for the Cenozoic tectonic evolution of western North America," *Geological Society of America Bulletin*, vol. 81, no. 12, pp. 3513–3536, 1970.

[154] J. Stock and P. Molnar, "Uncertainties and implications of the Late Cretaceous and Tertiary position of North America relative to the Farallon, Kula, and Pacific plates," *Tectonics*, vol. 7, no. 6, pp. 1339–1384, 1988.

[155] B. R. Hacker, A. Yin, J. M. Christie, and A. W. Snoke, "Differential stress, strain rate, and temperatures of mylonitization in the Ruby Mountains, Nevada: implications for the rate and duration of uplift," *Journal of Geophysical Research: Solid Earth*, vol. 95, no. B6, pp. 8569–8580, 1990.

[156] F. O. Marques, N. Mandal, S. Ghosh, G. Ranalli, and S. Bose, "Channel flow, tectonic overpressure, and exhumation of high-pressure rocks in the Greater Himalayas," *Solid Earth*, vol. 9, no. 5, pp. 1061–1078, 2018.

[157] F. O. Marques, G. Ranalli, and N. Mandal, "Tectonic overpressure at shallow depth in the lithosphere: the effects of boundary conditions," *Tectonophysics*, vol. 746, pp. 702–715, 2018.

[158] S. M. Schmalholz, S. Medvedev, S. M. Lechmann, and Y. Podladchikov, "Relationship between tectonic overpressure, deviatoric stress, driving force, isostasy and gravitational potential energy," *Geophysical Journal International*, vol. 197, no. 2, pp. 680–696, 2014.

[159] X. Chu, J. J. Ague, Y. Y. Podladchikov, and M. Tian, "Ultrafast eclogite formation via melting-induced overpressure," *Earth and Planetary Science Letters*, vol. 479, pp. 1–17, 2017.

[160] P. Yamato and J. P. Brun, "Metamorphic record of catastrophic pressure drops in subduction zones," *Nature Geoscience*, vol. 10, no. 1, pp. 46–50, 2017.

[161] C. Luisier, L. Baumgartner, S. M. Schmalholz, G. Siron, and T. Vennemann, "Metamorphic pressure variation in a coherent Alpine nappe challenges lithostatic pressure paradigm," *Nature communications*, vol. 10, no. 1, pp. 1–11, 2019.

[162] R. C. Fletcher, "Dramatic effects of stress on metamorphic reactions: COMMENT," *Geology*, vol. 43, no. 1, article e354, 2015.

[163] B. Hobbs and A. Ord, "Dramatic effects of stress on metamorphic reactions: COMMENT," *Geology*, vol. 43, no. 11, article e372, 2015.

[164] J. Wheeler, "Dramatic effects of stress on metamorphic reactions," *Geology*, vol. 42, no. 8, pp. 647–650, 2014.

[165] F. S. Spear, J. B. Thomas, and B. W. Hallett, "Overstepping the garnet isograd: a comparison of QuiG barometry and thermodynamic modeling," *Contributions to Mineralogy and Petrology*, vol. 168, no. 3, pp. 1–15, 2014.

[166] M. Seton, R. D. Müller, S. Zahirovic et al., "Global continental and ocean basin reconstructions since 200 Ma," *Earth-Science Reviews*, vol. 113, no. 3-4, pp. 212–270, 2012.

[167] D. C. Engebretson, A. Cox, and R. G. Gordon, "Relative motions between oceanic plates of the Pacific Basin," *Journal of Geophysical Research: Solid Earth*, vol. 89, no. B12, pp. 10291–10310, 1984.

[168] A. Crafford, *Geologic Map of Nevada: US Department of the Interior*, US Geological Survey Data Series, 2007.

[169] S. Dee, C. D. Henry, M. W. Ressel, and A. V. Zuza, "Preliminary geologic map of the north half of the Independence Valley NW quadrangle and the adjacent part of the Independence Valley NE quadrangle, Elko County, Nevada," Nevada Bureau of Mines and Geology Open File Report 17-6, scale 1:24,000, 2017.

[170] K. Min, R. Mundil, P. R. Renne, and K. R. Ludwig, "A test for systematic errors in ^{40}Ar/^{39} Ar geochronology through comparison with U/Pb analysis of a 1.1-Ga rhyolite," *Geochimica et Cosmochimica Acta*, vol. 64, no. 1, pp. 73–98, 2000.

[171] R. H. Steiger and E. Jager, "Subcommission on geochronology: convention on the use of decay constants in geo- and cosmochronology," *Earth and Planetary Science Letters*, vol. 36, no. 3, pp. 359–362, 1977.